1

2

3

4

5

6   **Neuronal hyperexcitability is a DLK-dependent trigger of HSV-1 reactivation that**

7   **can be induced by IL-1**

8

9   Sean Cuddy[1,2#], Austin R. Schinlever[1#], Sara Dochnal[1], Jon Suzich[1], Parijat Kundu[1],

10 Taylor K. Downs[3], Mina Farah[1], Bimal Desai[3], Chris Boutell[4] and Anna R. Cliffe[1*]

11

12

13   1. Department of Microbiology, Immunology and Cancer Biology, University of

14   Virginia, Charlottesville, VA, 22908.

15   2. Neuroscience Graduate Program, University of Virginia, Charlottesville, VA,

16   22908

17   3. Department of Pharmacology, University of Virginia, Charlottesville, VA, 22908.

18   4. MRC-University of Glasgow Centre for Virus Research (CVR), Garscube

19   Campus, Glasgow, Scotland, United Kingdom

20

21 # Denotes equal contribution

22

23 * Correspondence to Anna R. Cliffe, cliffe@virginia.edu

24

Abstract

Herpes Simplex Virus (HSV) establishes a latent infection in neurons and periodically reactivates to cause recurrent disease. The stimuli that act on neurons to trigger HSV reactivation have not been fully elucidated. Here we demonstrate that HSV reactivation is triggered by stimuli that induce neuronal hyperexcitability. Neuronal stimulation-induced reactivation was dependent on voltage-gated ion and hyperpolarization-activated cyclic nucleotide-gated (HCN) channels, demonstrating that neuronal activity is required for HSV reactivation. Hyperexcitability-induced reactivation was dependent on the neuronal specific pathway of DLK/JNK activation and progressed via an initial wave of viral gene expression that was independent of histone demethylase activity and linked to increased levels of histone phosphorylation. IL-1β induces neuronal hyperexcitability and is released under conditions of psychological stress and fever; both known triggers of clinical HSV reactivation. IL-1β treatment of sympathetic neurons induced histone phosphorylation, and importantly HSV reactivation, which was dependent on both DLK and neuronal excitability. Thus, HSV co-opts an innate immune pathway resulting from IL-1 stimulation of sympathetic neurons to induce reactivation from latency.

42

43

Introduction

Herpes simplex virus-1 (HSV-1) is a ubiquitous human pathogen that is present in approximately 40-90% of the population worldwide[1]. HSV-1 persists for life in the form of a latent infection in neurons, with intermittent episodes of reactivation. Reactivation from a latent infection and subsequent replication of the virus can cause substantial disease including oral and genital ulcers, herpes keratitis and encephalitis. In addition, multiple studies have linked persistent HSV-1 infection to the progression of Alzheimer's disease[2]. Stimuli in humans that are linked with clinical HSV-1 reactivation include exposure to UV light, psychological stress, fever and changes in hormone levels[3]. How these triggers result in reactivation of latent HSV-1 infection is not fully understood.

During a latent infection of neurons, there is evidence that the viral genome is assembled into a nucleosomal structure by associating with cellular histone proteins[4]. The viral lytic promoters have modifications that are characteristic of silent heterochromatin (histone H3 di- and tri-methyl lysine 9; H3K9me2/3, and H3K27me3)[5-8], which is thought to maintain long-term silencing of the viral lytic transcripts. Hence, for reactivation to occur, viral lytic gene expression is induced from promoters that are assembled into heterochromatin and in the absence of viral proteins, such as VP16, which are important for lytic gene expression upon *de novo* infection. Reactivation is therefore dependent on the host proteins and the activation of cellular signaling pathways[3]. However, the full nature of the stimuli that can act on neurons to trigger

66   reactivation and the mechanisms by which expression of the lytic genes occurs have

67   not been elucidated.

68

69   One of the best characterized stimuli of HSV reactivation at the cellular level is

70   nerve-growth factor (NGF) deprivation resulting from loss of PI3K/AKT activity[9-11].

71   Previously, we found that activation of activation of the c-Jun N-terminal kinase (JNK)

72   cell stress response via activation of dual leucine zipper kinase (DLK) was required for

73   reactivation in response to loss of NGF signaling. In addition, recent work has identified

74   a role for JNK in HSV reactivation following perturbation of the DNA damage/repair

75   pathways, which also trigger reactivation via inhibition of AKT activity[12]. DLK is a master

76   regulator of the neuronal stress response, and its activation can result in cell death,

77   axon pruning, axon regeneration or axon degeneration depending on the nature of

78   activating trigger[13,14]. Therefore, it appears that HSV has coopted this neuronal stress

79   pathway of JNK activation by DLK to induce reactivation. One key mechanism by which

80   JNK functions to promote lytic gene expression is via a histone phosphorylation on S10

81   of histone H3[15]. JNK-dependent histone phosphorylation occurs on histone H3 that

82   maintains K9 methylation and is therefore known as a histone methyl/phospho switch,

83   which permits transcription without the requirement for recruitment of histone

84   demethylases[16,17]. This initial wave of viral lytic gene expression is known as Phase I,

85   and also occurs independently of the lytic transactivator VP16. In addition, late gene

86   expression in Phase I occurs independent of viral genome replication[18,19]. A sub-

87   population of neurons then progress to full reactivation (also known as Phase II), which

88   occurs 48-72h post-stimulus and requires both VP16 and histone demethylase activity

89   [15,20-23]. However, not all models of reactivation appear to go through this bi-phasic

90   progression to reactivation as axotomy results in more rapid viral gene expression and

91   dependence on histone demethylase activity for immediate viral gene expression.

92

93   The aim of this study was to determine if we could identify novel triggers of HSV

94   reactivation and determine if they involved a bi-phasic mode of reactivation. We decided

95   to focus on stimuli that cause heightened neuronal activity because hyperstimulation of

96   cortical neurons following forskolin treatment or potassium chloride mediated

97   depolarization has previously been found to result in a global histone methyl/phospho

98   switch[24]. Whether this same occurs in different types of neurons, including sympathetic

99   neurons, is not known. Although forskolin has previously been found to induce HSV

100   reactivation,[25-28], whether this is a result of inducing hyperexcitability or as a

101   consequence of activation of alterative cAMP-responsive proteins including PKA and

102   CREB is not known. Therefore, we investigated if forskolin-mediated reactivation was a

103   result of increased neuronal activity. Hyperexcitability of neurons is correlated with

104   changes in cellular gene expression, increased DNA damage[29,30] and epigenetic

105   changes including H3 phosphorylation[24]. However, DLK-mediated activation of JNK has

106   not been linked to changes in cellular gene expression in response to hyperexcitability.

107   Therefore, we were also interested in determining whether DLK and JNK are required

108   for induction of HSV gene expression in response to hyperexcitability.

109

110   IL-1β is released under conditions of psychological stress and fever[31-34]; both

111   known triggers of clinical HSV reactivation[35-38]. IL-1β has previously been found to

112   induce heightened neuronal activity[39-41]. However, an intriguing feature of IL-1β

113   signaling is its ability to have differential effects on different cell types. For example, IL-

114   1β is involved extrinsic immune response to infection via activation of neutrophils and

115   lymphocytes. In addition, it can act on non-immune cells including fibroblasts to initiate

116   an antiviral response[42,43], as has previously been described for lytic infection with HSV-

117   1[42]. Given these differential downstream responses to IL-1β signaling, we were

118   particularly interested in the effects of IL-1β treatment of latently infected neurons.

119   Interestingly, we found that IL-1β was capable of inducing reactivation of HSV from

120   mature sympathetic neurons. Inhibition of voltage-gated sodium and hyperpolarization

121   activated cyclic nucleotide gated (HCN) channels prevented reactivation mediated by

122   both forskolin and IL-1β. Activity of the cell stress protein DLK was also essential for IL-

123   1β-mediated reactivation. We therefore identify IL-1β as a novel trigger from HSV

124   reactivation that acts via neuronal hyperexcitability and highlight the central role of JNK

125   activation by DLK in HSV reactivation.

126

127   **Results**

128   Adenylate Cyclase Activation Triggers DLK/JNK-Dependent Reactivation of HSV from

129   Latent Infection in Sympathetic Neurons
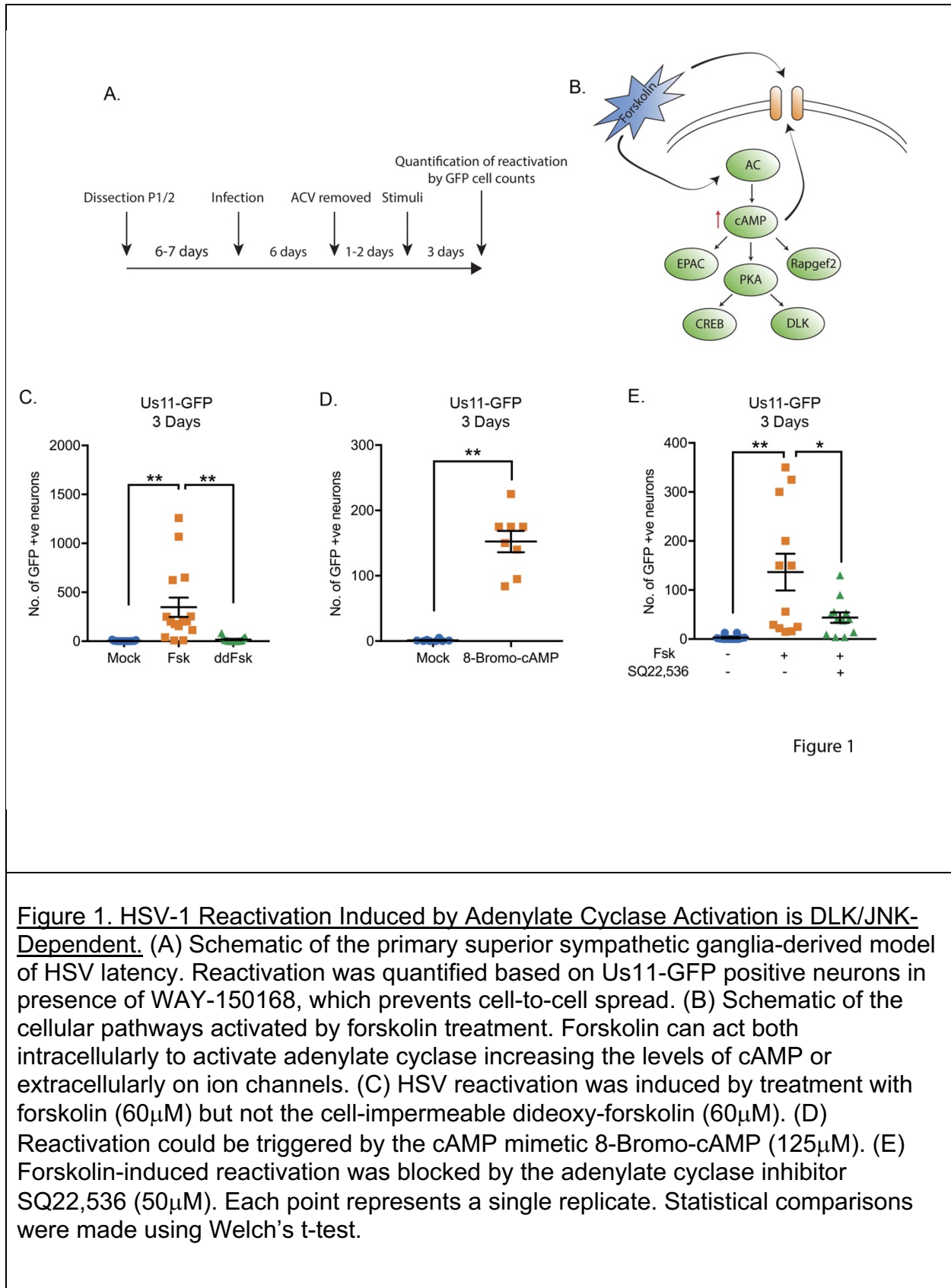
130   Both forskolin and cAMP mimetics are well known to induce neuronal

131   hyperexcitation and have previously also been found to trigger HSV reactivation[25-28].

132   Using a model of HSV latency in mouse sympathetic neurons isolated from the super-

133   cervical ganglia (SCG)[15] we investigated whether forskolin treatment induced

134   reactivation in this system and the potential mechanism resulting in the initial induction

135   of viral lytic gene expression. Sympathetic SCG neurons were infected with a Us11-

136   GFP tagged HSV-1[44] at a multiplicity of infection (MOI) of 7.5 PFU/cell in the presence

137   of acyclovir (ACV). After 6 days the ACV was washed out and the neuronal cultures

138   monitored to ensure that no GFP-positive neurons were present. Two days later,

139   reactivation was triggered by addition of forskolin (Figure 1A). As represented in figure

140   1B, forskolin can act either extra-cellularly on ion channels or intracellularly to activate

141   adenylate cyclase[45-47]. Dideoxy-forskolin is a cell impermeable forskolin analog that can

142   act directly on voltage gated ion channels but does not activate cAMP[45,48]. We found

143   addition of forskolin but not dideoxy-forskolin triggered HSV reactivation (Figure 1C). In

144   addition, treatment of latently infected primary neurons with a cAMP mimetic (8-bromo-

145   cAMP) was sufficient to trigger reactivation (Figure 1D) and inhibition of adenylate

146   cyclase activity using SQ22, 536[49] significantly diminished HSV reactivation (Figure 1E).

147   Therefore, activation of adenylate cyclase activation and subsequent increased

148   intracellular levels of cAMP are required for forskolin-mediated reactivation.

149

150   DLK/JNK Activity is Required for the Early Phase of Viral Gene Expression in Response

151   to Forskolin Treatment

152   We previously found that DLK-mediated JNK activation was essential for Phase I

153   reactivation following interruption of nerve growth factor signaling. To determine

154   whether DLK and JNK activation were crucial for reactivation in response to

155   hyperexcitability, neurons were reactivated with forskolin in the presence of the JNK-

156   inhibitor SP600125 (Fig. 2A) or the DLK inhibitor GNE-3511[50] (Fig. 2B), which

157   prevented reactivation based on the number of GFP-positive neurons at 3-days post-

Figure 1. HSV-1 Reactivation Induced by Adenylate Cyclase Activation is DLK/JNK-Dependent. (A) Schematic of the primary superior sympathetic ganglia-derived model of HSV latency. Reactivation was quantified based on Us11-GFP positive neurons in presence of WAY-150168, which prevents cell-to-cell spread. (B) Schematic of the cellular pathways activated by forskolin treatment. Forskolin can act both intracellularly to activate adenylate cyclase increasing the levels of cAMP or extracellularly on ion channels. (C) HSV reactivation was induced by treatment with forskolin (60μM) but not the cell-impermeable dideoxy-forskolin (60μM). (D) Reactivation could be triggered by the cAMP mimetic 8-Bromo-cAMP (125μM). (E) Forskolin-induced reactivation was blocked by the adenylate cyclase inhibitor SQ22,536 (50μM). Each point represents a single replicate. Statistical comparisons were made using Welch's t-test.

158   reactivation Inhibition of either JNK or DLK blocked HSV reactivation in response to

159   forskolin. These data therefore indicate hyperexcitability-induced reactivation is

160   dependent on the neuronal stress pathway mediated by DLK activation of JNK.

161

162   Because we previously found that JNK-activation results in a unique wave of viral

163   gene expression in response to inhibition of nerve-growth factor signaling, we especially

164   intrigued to determine whether hyperexcitability triggers a similar wave of JNK

165   dependent viral gene expression. The previously described bi-phasic progression to

166   viral reactivation is characterized by viral DNA replication and production of infectious

167   virus, occurring around 48-72 post-stimulus[18], but an earlier wave of lytic gene

168   expression occurring around 20h post-stimulus. To determine whether forskolin-

169   mediated reactivation results in a similar kinetics of reactivation, we investigated the

170   timing of Us11-GFP synthesis, viral DNA replication, production of infectious virus and

171   lytic gene induction following forskolin treatment. In response to forskolin treatment,

172   GFP synthesis in neurons started to appear around 48h post-reactivation, with more

173   robust reactivation observed at 72h (Figure 2C). In contrast to forskolin-mediated

174   reactivation, the number of GFP-positive neurons following superinfection with a

175   replication competent wild-type virus resulted in a rapid induction of GFP-positive

176   neurons by 24h post-superinfection (Figure 2C). Therefore, forskolin triggered

177   reactivation results in slower synthesis of Us11-GFP than superinfection. In addition,

178   these data highlight the ability of forskolin to trigger reactivation from only a

179   subpopulation of latently infected neurons (approximately 1 in every 3.4 neurons
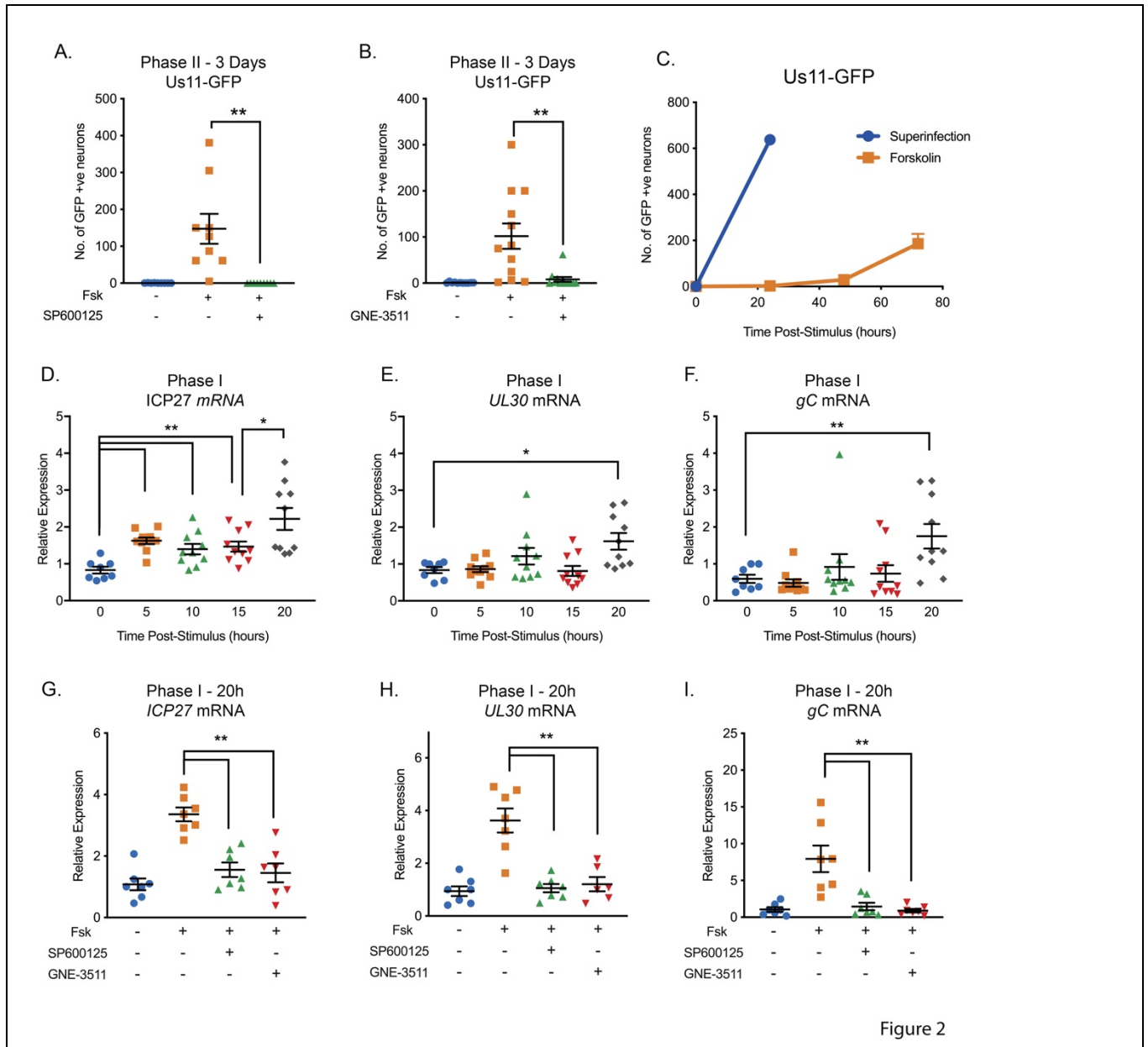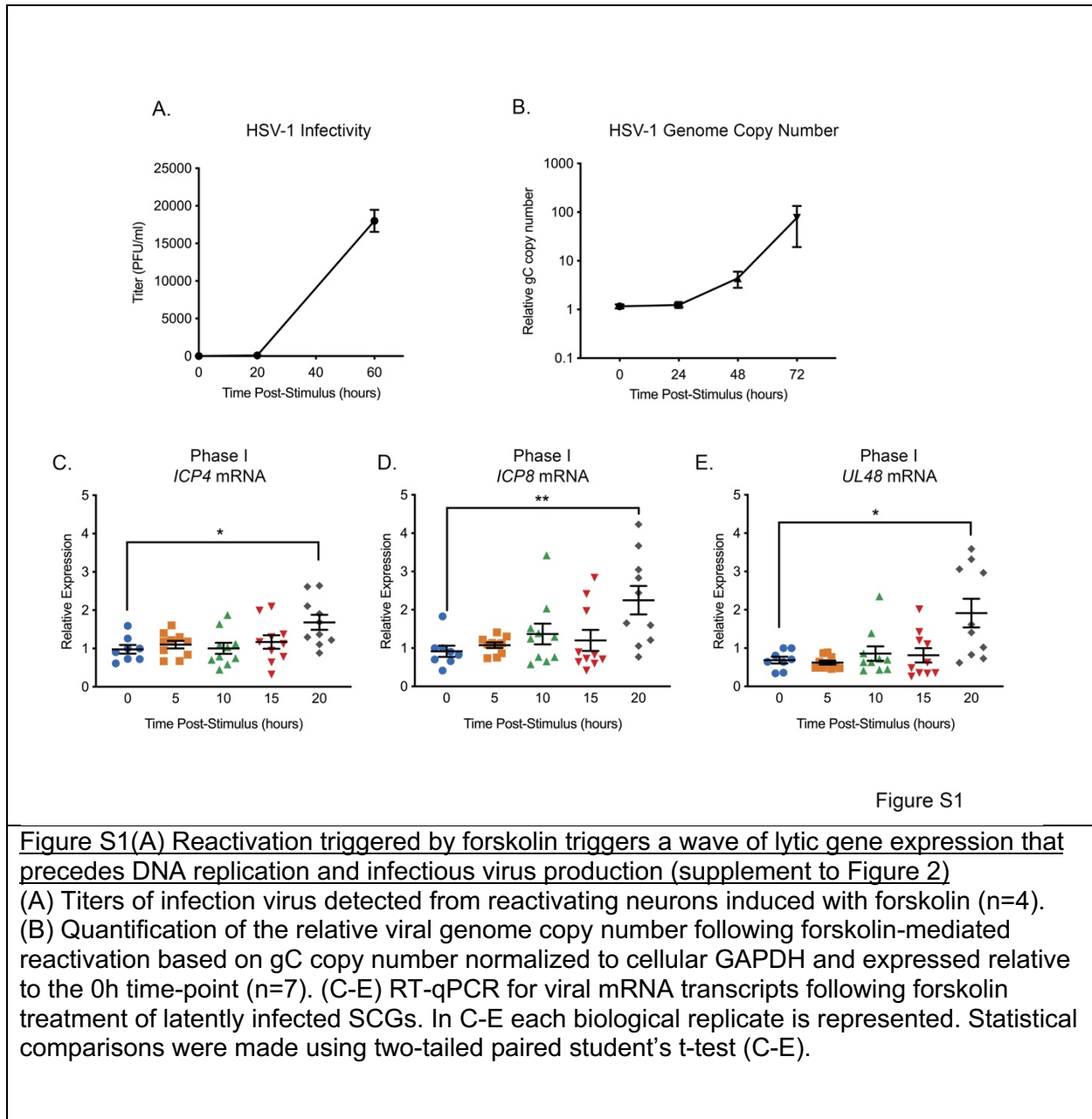
180   compared to superinfection).

Figure 2. Reactivation Triggered by Forskolin Involves a DLK/JNK Dependent Phase I of Viral Gene Expression.

(A) Reactivation was induced by forskolin in the presence of JNK inhibitor SP600125 (20µM). (B) Reactivation was induced by forskolin in the presence of the DLK inhibitor GNE-3511 (4µM). (C) Reactivation was induced by forskolin or superinfection with a wild-type (F strain) HSV-1 (MOI of 10 PFU/cell) and qualified based on Us11-GFP positive neurons (n=3). (D-F) RT-qPCR for viral mRNA transcripts following forskolin treatment of latently infected SCGs. (G-I) RT-qPCR for viral lytic transcripts at 20h post-forskolin treatment and then in presence of the JNK inhibitor SP600125 (20µM) and the DLK inhibitor GNE-3511 (4µM). In D-L each experimental replication is represented. Statistical comparisons were made using two-tailed paired student's t-test.

181

182

Figure S1

Figure S1(A) Reactivation triggered by forskolin triggers a wave of lytic gene expression that precedes DNA replication and infectious virus production (supplement to Figure 2)
(A) Titers of infection virus detected from reactivating neurons induced with forskolin (n=4).
(B) Quantification of the relative viral genome copy number following forskolin-mediated reactivation based on gC copy number normalized to cellular GAPDH and expressed relative to the 0h time-point (n=7). (C-E) RT-qPCR for viral mRNA transcripts following forskolin treatment of latently infected SCGs. In C-E each biological replicate is represented. Statistical comparisons were made using two-tailed paired student's t-test (C-E).

183

184

185   The production of infectious virus also mirrored the data for the detection of

186   Us11-GFP positive neurons, with a robust increase in viral titers between 24 and 60h

187   post-stimulus (Figure S1A). An increase in viral genome copy was also not detected

188   until 48h post-stimulus, which continued between 48h and 72h (Figure S1B). The

189   quantification of viral genome copy number was also carried out in presence of WAY-

190   150138[51], which prevents packaging of the viral genome[52], therefore indicating that

191   DNA replication occurs in reactivating neurons and not as a consequence of cell-to-cell

192   spread.

193

194   Given the observed 48h delay in viral DNA replication and production of

195   infectious virus, we were interested to determine if there was a Phase I wave of lytic

196   gene expression that occurred prior to viral DNA replication. We therefore carried out

197   RT-qPCR to detect representative immediate-early (*ICP27* and *ICP4*), early (*ICP8* and

198   *UL30*) and late (*UL48* and *gC*) transcripts between 5- and 20-hours post addition of

199   forskolin (Figures 2D-F and S1C-E). For all six transcripts, a significant up-regulation of

200   mRNA occurred at 20h post-treatment, including the true late gene *gC*, whose

201   expression would usually only be stimulated following viral genome replication in the

202   context of *de novo* lytic replication. Therefore, this indicates that lytic gene expression is

203   induced prior to viral DNA replication and that neuronal hyperexcitability does trigger a

204   Phase I wave of lytic gene expression. Notably, we did detect small but reproducible

205   induction of *ICP27* mRNA at 5h post-stimulus, followed by a second induction at 20h

206   (Figure 2D), indicating that there is likely differential regulation of some viral lytic

207   transcripts during Phase I reactivation induced by hyperexcitability that is distinct from

208   both NGF-deprivation and *de novo* lytic infection.

209

210   To determine whether JNK and DLK were required Phase I gene expression in

211   response to hyperexcitability, we investigated viral mRNA levels following forskolin-

212   mediated reactivation in the presence of the JNK inhibitor SP600125. We found a

213   significant reduction in *ICP27* (2.2-fold), *UL30* (3.3-fold) and *gC* (5.5-fold) mRNA levels

214   at 20h post-stimulus in the presence of SP600125 (Figure 2J-L). For all genes tested,

215   there was no significant increase in mRNAs in the JNK-inhibitor treated neurons

216   compared to mock. We observed comparable results following treatment with the DLK

217   inhibitor GNE-3511, with a 2.3-, 3-, 8.8-fold decrease in *ICP27*, *UL30* and *gC* mRNAs

218   respectively compared to forskolin treatment alone, and no significant increase in

219   mRNA levels compared to the reactivated samples (Figure 2J-L).

220

221   It is possible that in addition to JNK, other signal transduction proteins are

222   important in forskolin-mediated reactivation. Previous data has found that DLK can be

223   activated by PKA, which is well known to be activated by cAMP. However, using well

224   characterized inhibitors of PKA, along with the PKA-activated transcription factors

225   CREB, in addition to two other cAMP responsive proteins Rapgef2 and EPAC, we did

226   not find that these cAMP activated proteins were required for Phase I reactivation

227   (Figure S2). Inhibition of PKA or CREB did reduce Phase II reactivation (Figure S2A

228   and C) but had no effect on Phase I (Figure S2B and D). Inhibition of Rapgef2 or PEAC

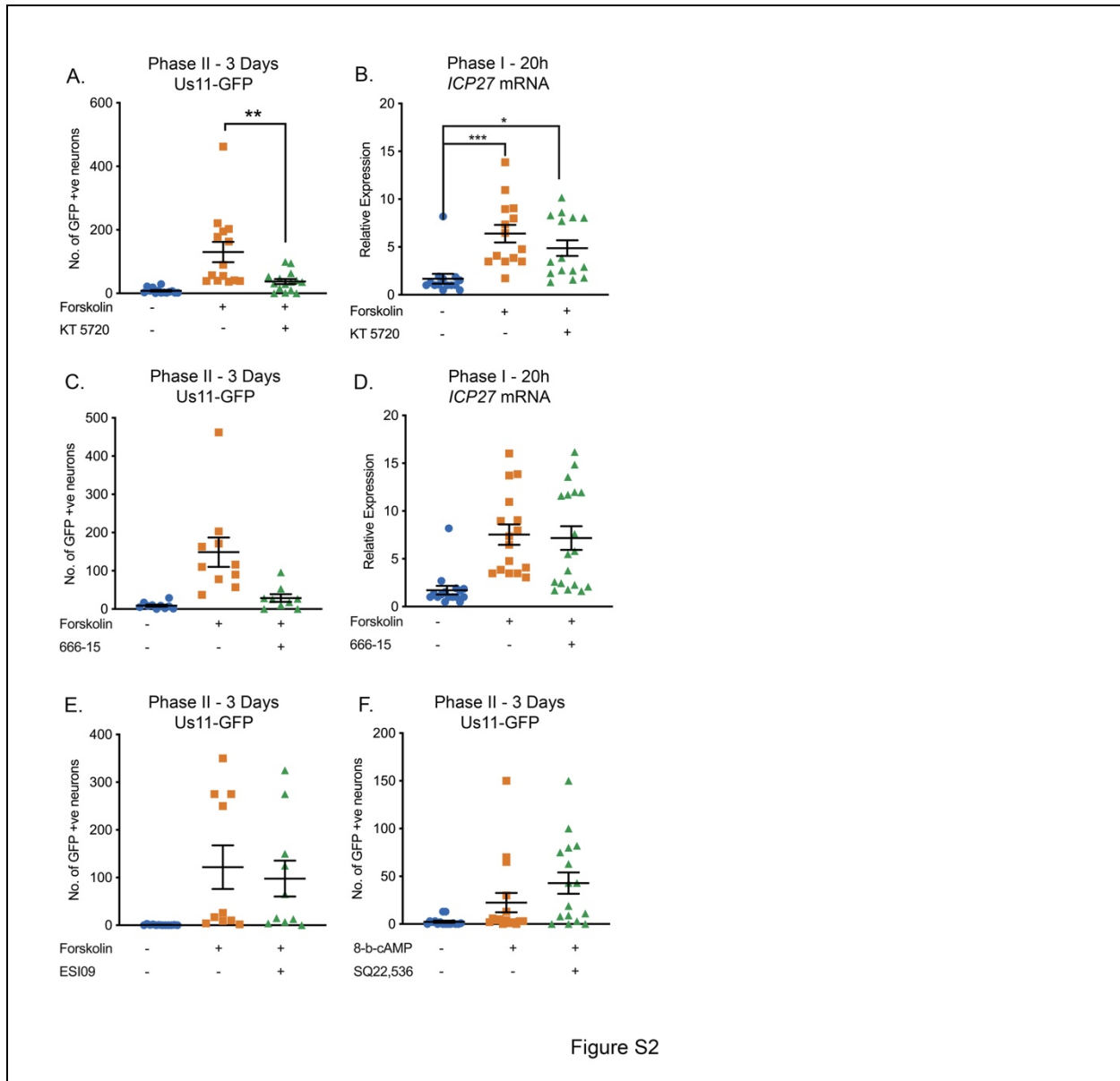229   had no effect on HSV reactivation (Figure SE and F). Taken together, these data

Figure S2

Figure S2. Effect of PKA, CREB, Rapgef2 and EPAC Inhibition on HSV-1 Reactivation. (A) Latently infected cultures were reactivated with forskolin (60 μM) in the presence of the PKA inhibitor KT 5720 (3 μM) and the number of Us11-GFP positive neurons quantified at 3 days post-reactivation. (B) RT-qPCR for the viral lytic transcript ICP27 at 20h post-forskolin treatment and in the presence of KT 5720. (C) Latently infected cultures were reactivated with forskolin in the presence of the CREB inhibitor 666-15 (2 μM). (D) RT-qPCR for ICP27 at 20h post-forskolin treatment and in the presence of 666-15. (E) Latently infected cultures were reactivated with forskolin (60μM) in the presence of the EPAC inhibitor ESI09 (10 μM). (F) Latently infected cultures were reactivated with 8-Bromo-cAMP (125μM) in the presence of the Rapgef2 inhibitor SQ22,536 (50 μM). Individual experimental replicates are represented. Statistical comparisons were made using Welch's t-test (A) or two-tailed unpaired t-test (B).

230

231

232   indicate that it is hyperexcitability induced by forskolin that induces a Phase I wave of

233   gene expression via activation of DLK and JNK.

234

235   <u>Forskolin Triggers a Phase-I Wave of Viral Gene Expression that is Independent of</u>

236   <u>Histone Demethylase Activity.</u>

237   Hyperexcitability results in the propensity of neurons to fire repeated action

238   potentials, and is associated with specific changes in histone posttranslational

239   modifications. The first is physiological DNA damage[29,30], measured by the intensity of

240   γH2AX staining in neuronal nuclei. Forskolin treatment was associated with an increase

241   in the levels of γH2AX at 5h post-treatment, which resolved by 15h post-treatment

242   (Figure S2A and C), and is therefore indicative of physiological DNA damage and

243   repair, which occurs upon neuronal hyperexcitability. A second reason for probing the

244   DNA damage/repair pathway in response to forskolin treatment is that previously

245   reactivation of HSV from latency has been associated with perturbation of the DNA

246   damage/repair response[12]. Both inhibition of repair and exogenous DNA damage

247   resulted in loss of AKT phosphorylation by PHLPP1, which was required for HSV

248   reactivation. Although we did observe increased levels of γH2AX following forskolin

249   treatment, this was not accompanied by a loss of pAKT measured at 15h post-treatment

250   (Figure S2D). This indicates that HSV reactivation in response to forskolin treatment

251   does not involve dephosphorylation of AKT. Therefore, hyperexcitability triggers

252   reactivation via an alternative mechanism that does not feed into the AKT.
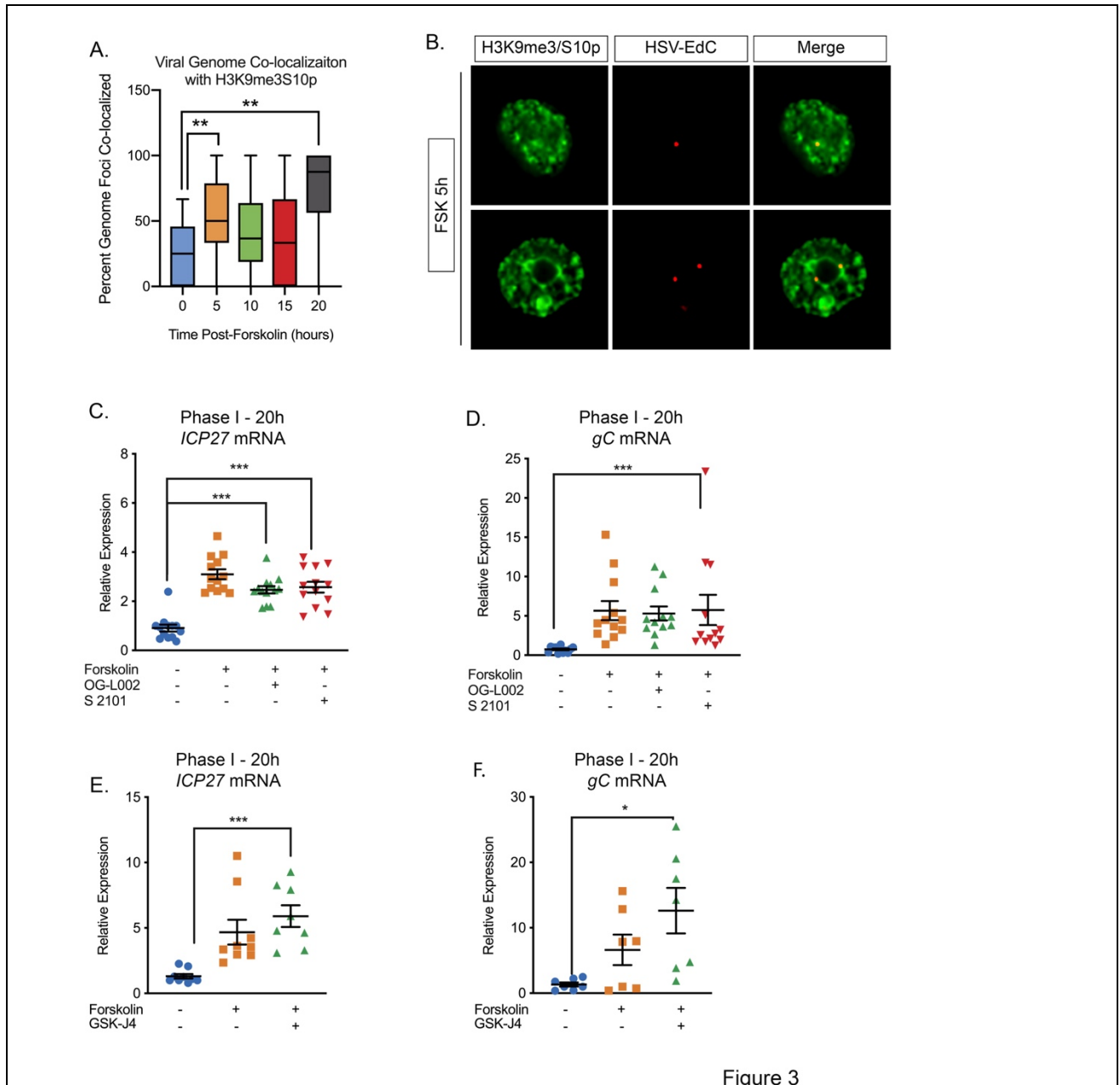
253

Figure 3. The Initial Wave of Viral Lytic Gene Expression During Forskolin-mediated Reactivation is Independent on Histone Demethylase Activity. (A) Quantification of the percentage of genome foci stained using click-chemistry that co-localize with H3K9me3/S10p. At least 15 fields of view were blindly scored from two independent experiments. Whiskers represent the 2.5-97.5 percentile range. (B) Representative images of click-chemistry based staining of HSV-EdC genomes and H3K9me3/S10p staining at 5h post-forskolin treatment. (C and D). Effect of the LSD1 inhibitors OG-L002 and S 2101 on forskolin-mediated Phase I of reactivation determined by RT-qPCR for ICP27 (C) and gC (D) viral lytic transcripts at 20h post-forskolin treatment and in the presence of 15μM OG-L002 and 20μM S 2102. (E) Effect of the JMJD3 and UTX inhibitor GSK-J4 (2μM) on forskolin-mediated Phase I measured by RT-qPCR for viral lytic transcripts ICP27 (E) and gC (F) at 20h post-forskolin treatment and in the presence of GSK-J4. For C-F each experimental replicate is represented. Statistical comparisons were made using two-tailed unpaired t-test (A) or Welch's t-test (C-F).
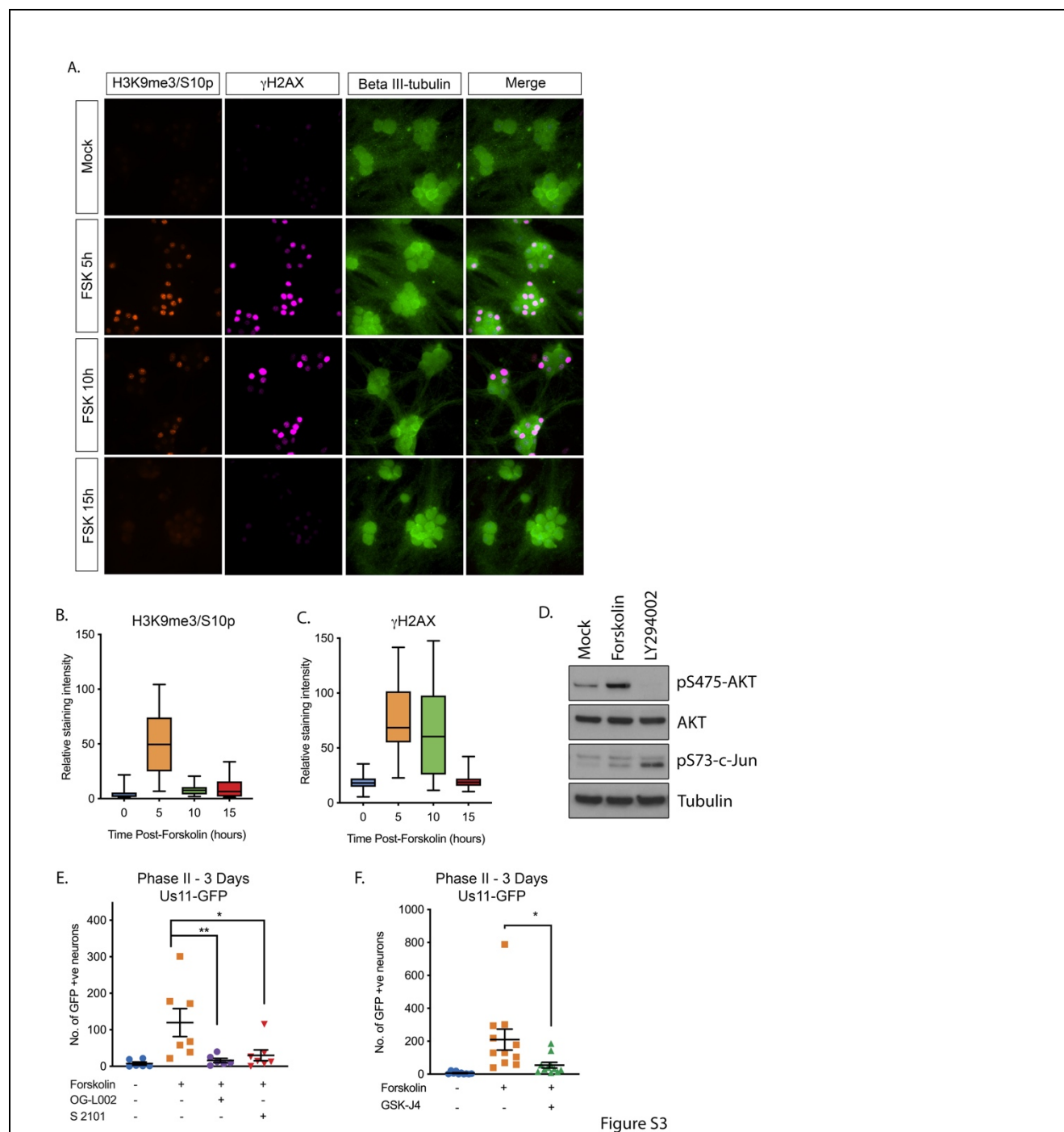
Figure S3. Forskolin Treatment Induces Hyperexcitability-associated Histone Post-translational Modification in Sympathetic Neurons. SCG neurons were treated with forskolin and immunofluorescence staining was carried out for H3K9me3/S10p, the DNA damage marker γH2AX and the neuronal marker beta III-tubulin. (B) Quantification of neuronal nuclear staining intensity for H3K9me3 (>150 cells/condition). (C) Quantification of neuronal nuclear staining for γH2AX. In B and C, whiskers represent the 2.5-97.5 percentile range. (D). Western blotting for pS475-AKT, total AKT, pS73-c-Jun and tubulin at 15h post-treatment with the PI3-kinase inhibitor LY294002 (20μM) or forskolin (60 μM). (E) Effect of the LSD1 inhibitors OG-L002 (15μM) and S 2101 (20μM) on forskolin-mediated reactivation measured by Us11-GFP positive neurons. (F) Effect of the JMJD3

254

and UTX inhibitor GSK-J4 (2μM) on forskolin-mediated reactivation measured by Us11-GFP positive neurons. Statistical comparisons were made using Welch's t-test (E, F).

255   Previously, we found that Phase I reactivation is accompanied with a JNK-

256 dependent histone methyl/phospho (marked by H3K9me3/pS10) switch on lytic

257 promoters[15]. In cortical neurons, one study has found that hyperexcitability results in

258 increased H3K9me3/pS10[24]. Therefore, we were particularly interested to determine

259 whether forskolin treatment of sympathetic neurons triggered a histone S10

260 phosphorylation on H3K9me3. Forskolin triggered a transient increase in

261 H3K9me3/S10p at 5h post-treatment that had returned to baseline by 10h (Figure S3A

262 and B). This indicates that, in keeping with cortical neurons, forskolin induces a histone

263 H3K9me3/pS10 methyl/phospho switch on regions on cellular chromatin.

264

265   We next sought to determine whether the phospho/methyl switch that arises as a

266 result of hyperexcitability plays a role in Phase I of HSV reactivation. We therefore

267 investigated whether viral genomes were co-localized with H3K9me3/S10p following

268 forskolin treatment. To visualize HSV genomes, viral stocks were grown in the presence

269 of EdC as described previously[53,54]. Click-chemistry was performed on latently infected

270 and neurons following forskolin treatment. As shown in Figure 3A and B, viral genomes

271 co-localized with H3K9me3/pS10 following robust H3K9me3/S10p staining at 5h. The

272 percentage of viral genomes that co-localized with H3K9me3/S10p was significantly

273 increased compared to the unreactivated samples at 5h and 20h post-forskolin

274 treatment (Figure 3A).

275

276   Serine phosphorylation adjacent to a repressive lysine modification is thought to

277   permit transcription without the removal of the methyl group[17,24]. Therefore, we

278   investigated whether histone demethylase activity was required for the initial induction in

279   lytic gene expression following forskolin treatment. Previously, the H3K9me2 histone

280   demethylase LSD1 has been found to be required for full HSV reactivation[20,23], and in

281   our in vitro model this was determined by the production of infectious viral particles or

282   late gene synthesis at 48-72h post-reactivation[15]. Addition of two independent LSD1

283   inhibitors (OG-L002 and S 2102) inhibited Us11-GFP synthesis at 72h post-reactivation

284   (Figure 3C). Hence, LSD1 activity, and presumably removal of H3K9-methylation is

285   required for forskolin-mediated reactivation. However, LSD1 inhibition did not prevent

286   the initial induction of *ICP27* and *g*C mRNA expression at 20h post-forskolin treatment

287   (Figure 3D and E). Therefore, this initial wave of viral lytic gene expression following

288   forskolin-mediated reactivation is independent of histone H3K9 demethylase activity.

289

290   We previously found that H3K27me demethylase activity is required for full

291   reactivation but not the initial wave of gene expression[15]. However, because of the lack

292   of an antibody that specifically recognizes H3K27me3S28p and not also

293   H3K9me3S10p, we are unable at this point to investigate genome co-localization with

294   this combination of modifications. However, we could investigate the role of the

295   H3K27me demethylases in forskolin-mediated reactivation. Treatment of neurons with

296   the UTX/JMJD3 inhibitor GSK-J4[55] prevented the synthesis of Us11-GFP at 72h post-

297   reactivation, indicating that removal of K27 methylation is required full reactivation

298   (Figure 3F). However, the initial burst of gene expression (assessed by *ICP27* and *g*C

299   mRNA levels) was robustly induced at 20h post-forskolin treatment in the presence of

300   GSK-J4 (Figure 3G and H). Taken together, our data indicate that the initial phase of

301   gene expression following forskolin treatment is independent of histone demethylase

302   activity and therefore consistent with a role for a histone methyl/phospho switch in

303   permitting lytic gene expression.

304

305   Forskolin-Mediated Reactivation Requires Neuronal Excitability

306   Given that the HSV genome co-localized with regions of hyperexcitability-induced

307   changes in histone phosphorylation, we investigated whether reactivation was linked to

308   neuronal excitability. To inhibit action potential firing, we treated neurons with

309   tetrodotoxin (TTX), which inhibits the majority of the voltage gated sodium channels and

310   therefore depolarization. Addition of TTX significantly inhibited HSV reactivation

311   triggered by forskolin, as measured by Us11-GFP positive neurons at 72 hours post-

312   stimulus (Figure 4A). To further confirm a role for repeated action potential firing in

313   forskolin-mediated reactivation, we investigated the role of voltage gated potassium

314   channels, which are required for membrane repolarization. Addition of TEA, which

315   inhibits voltage-gated potassium channel activity, also blocked HSV reactivation

316   measure by Us11-GFP positive neurons at 3 days post-forskolin treatment (Figure S4B.

317   Taken together, these data indicate that action potential firing is required for forskolin-

318   mediated reactivation.

319

320   Increased levels of cAMP can act on nucleotide gated ion channels, including the

321   hyperpolarization activated cyclic nucleotide gated (HCN) channels. HCN channels are
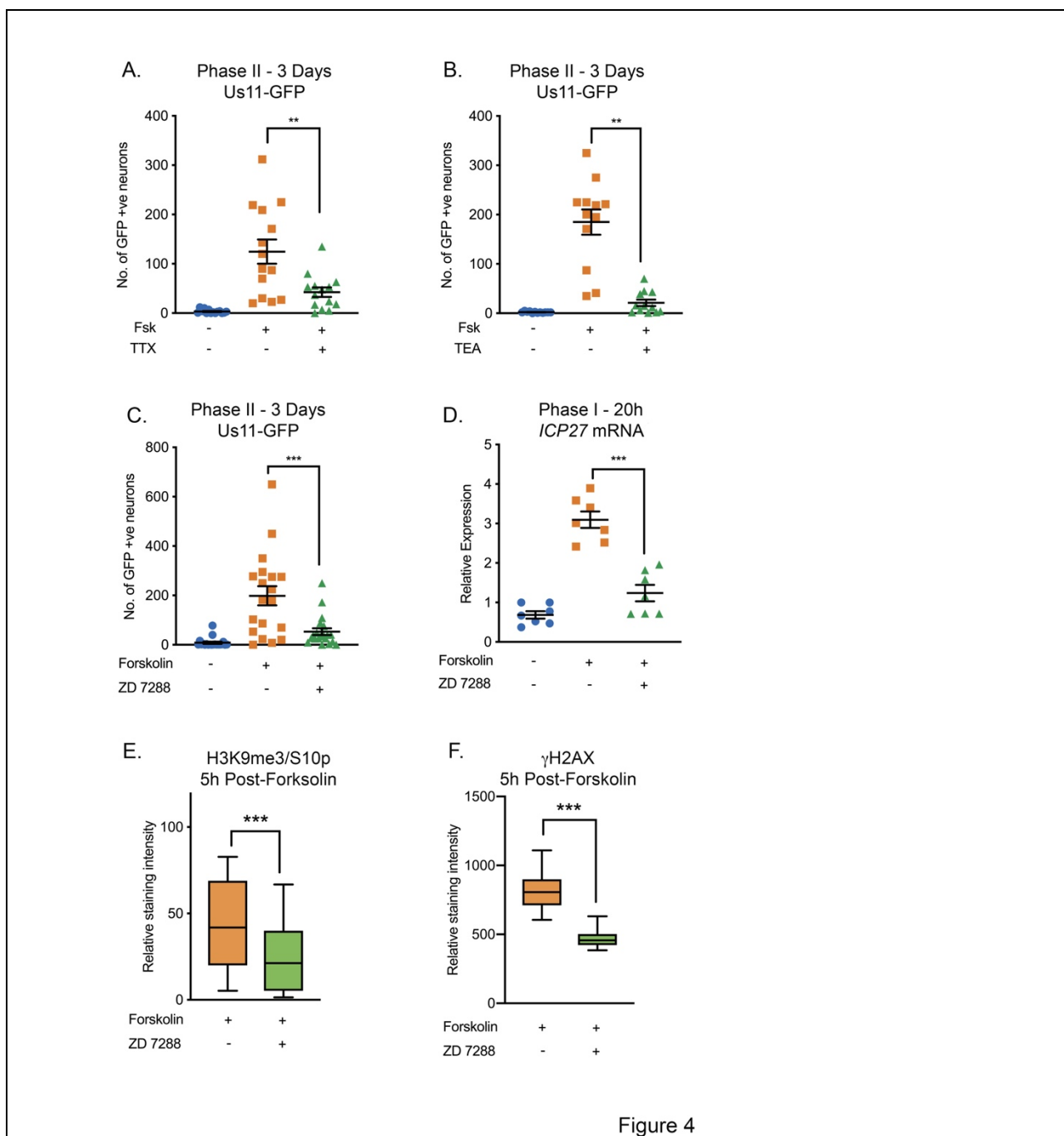
Figure 4

Figure 4. HSV Reactivation Mediated by Forskolin Requires Neuronal Activity.
(A) Latently infected cultures were reactivated with forskolin in the presence of the voltage-gated sodium channel blocker tetrodotoxin (TTX; 1μM) and the number of Us11-GFP positive neurons quantified at 3 days post-reactivation. (B) Latently infected cultures were reactivated with forskolin in the presence of the voltage-gated potassium channel blocker Tetraethylammonium (TEA; 10 mM) and the number of Us11-GFP positive neurons quantified at 3 days post-reactivation. (C) Forskolin-mediated reactivation in the presence of the HCN channel blockers ZD 7288 (10μM) quantified as the numbers of Us11-GFP positive neurons at 3 days post-reactivation. (D) The effect of ZD 7288 on the HSV lytic gene transcript ICP27 during Phase I reactivation measured at 20h post-forskolin treatment by RT-qPCR. Individual experimental

replicates are represented. (E and F) Quantification of the relative nuclear staining for H3K9me3/S10p and γH2AX in SCG neurons at 5h post-forskolin treatment and in the presence of ZD 7288 from two independent experiments. Statistical comparisons were made using Welch's t-test (A-C), two-tailed unpaired t-test (D-F).

322   K$^+$ and Na$^+$ channels that are activated by membrane hyperpolarization[56,57]. In the

323   presence of high levels of cAMP, the gating potential of HCN channels is shifted in the

324   positive direction, such that HCN channels can open at resting membrane potential,

325   resulting in an increased propensity of neurons to undergo repeated firing[57-59]. HCN

326   channel activity can be blocked by ZD 7288, Ivabradine or cesium chloride. Addition of

327   ZD 7288 (Figure 4A), Ivabradine (Figure S4A) or CsCl (Figure S4B) all significantly

328   reduced HSV reactivation triggered by forskolin, as measured by Us-11 GFP positive

329   neurons at 3 days post-stimulus. To determine whether HCN channel activity was

330   required for the initial induction of HSV lytic mRNA expression, we assessed viral

331   mRNA expression during Phase I in the presence and absence of ZD 7288. Expression

332   of representative lytic mRNAs *ICP27* (Figure 4D), *UL30* and *gC* (Figure S4C and D)

333   were significantly decreased in the presence of ZD 7288 compared to the forskolin

334   treated neurons alone, and were not significantly increased compared to the mock

335   treated samples. Therefore, HCN channel activity is required for the initial induction of

336   lytic gene expression during Phase I reactivation mediated by forskolin.

337

338   We also confirmed that inhibition of HCN-channel activity affected the levels of

339   hyperexcitability-associated changes in histone post-translational modifications.

340   Addition of ZD 7288 resulted in significantly decreased staining intensities of both

341   H3K9me3/S10p and γH2AX at 5h post-forskolin treatment (Figure 4F and G), which was

342   the peak time-point for which we observed these changes upon forskolin treatment

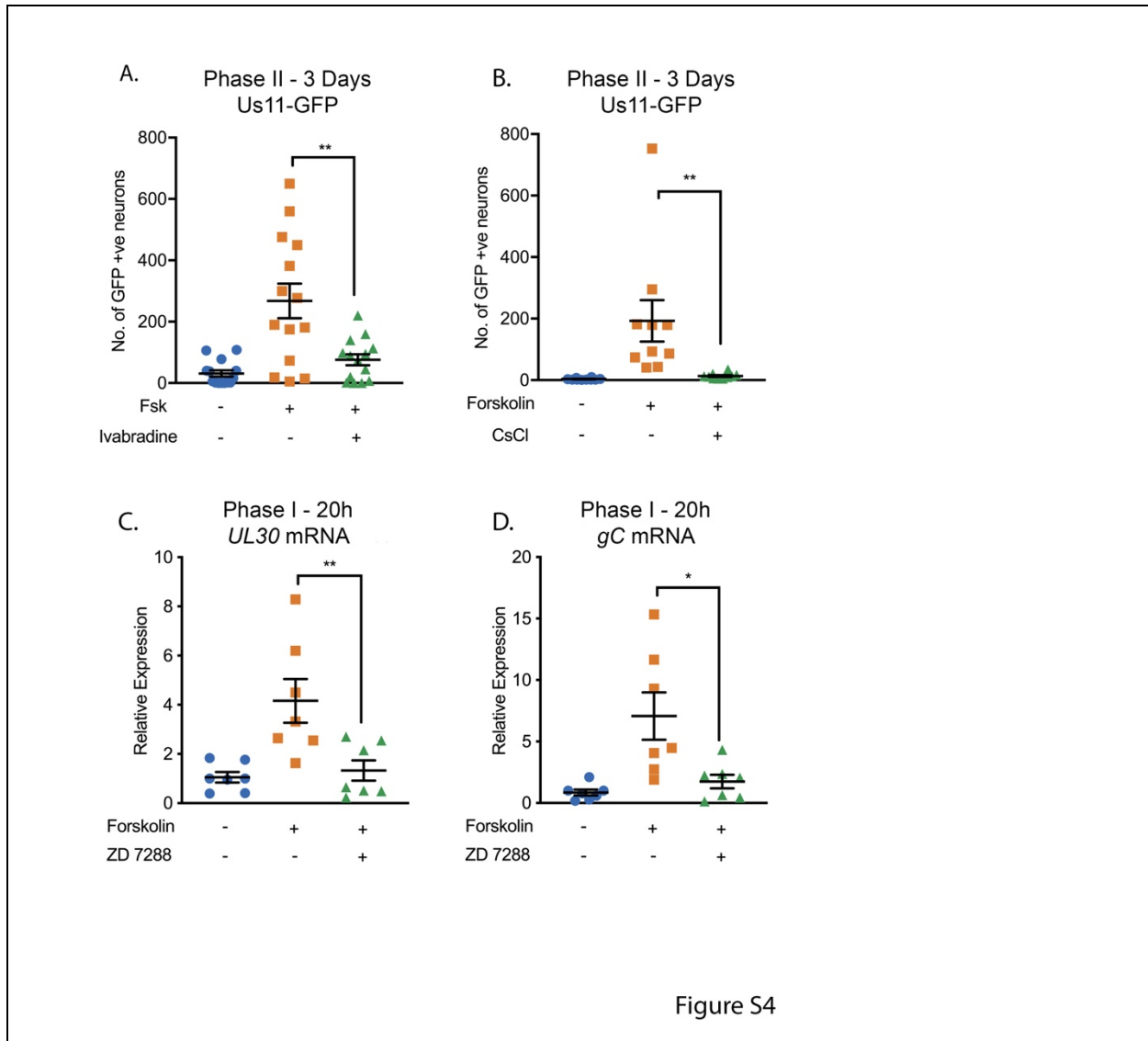343   alone (Figure S3 A and B). Therefore, activity of the HCN channels in response to

Figure S4

Figure S4. HSV Reactivation Mediated by Forskolin Requires Neuronal Activity. (A and B) Latently infected cultures were reactivated with forskolin in the presence of the HCN channel inhibitors ivabradine (20µM; A) and CsCl (3mM; B). Latently infected cultures were reactivated with forskolin in the presence of the HCN inhibitor ZD 7288 (10 µM) and viral lytic transcripts measured at 20h post-reactivation. Individual experimental replicates are represented. Statistical comparisons were made using Welch's t-test (A, B) or two-tailed unpaired t-test (C, D).

344

345

346   increased levels of cAMP results in hyperexcitability-associated changes in

347   histone modifications and reactivation of HSV from latent infection.

348

349   <u>HSV Reactivation can be Induced by Stimuli that Directly Increase Neuronal Excitability</u>

350   The role of ion-channel activity in forskolin-mediated reactivation prompted us to

351   investigate whether additional stimuli that induce hyperexcitability in neurons also

352   trigger HSV reactivation. We were also interested in whether reactivation required

353   chronic versus short term hyperexcitability. Increasing the extracellular concentration of

354   KCl is well-known to induce action potential firing. Therefore, we investigate the timing

355   of both KCl and forskolin-mediated hyperexcitability in HSV reactivation. Both of these

356   treatments triggered HSV reactivation more robustly if applied for 8h or more (Figure

357   5A). This indicates that chronic neuronal hyperactivity is important in inducing

358   reactivation of HSV.

359

360   To further clarify that hyperexcitability can directly trigger HSV reactivation, we

361   investigated the effects of removal from a TTX block on latently infected neurons.

362   Addition of TTX to neurons results in synaptic scaling, so that when the TTX is removed

363   the neurons enter a hyperexcitable state[60-63]. TTX was added to the neurons for 2 days

364   and then washed out. This resulted in a robust HSV reactivation as determined by

365   Us11-GFP synthesis (Figure 5B). We also investigated whether the JNK-cell stress

366   pathway was important in HSV reactivation in response to TTX-release. Addition of the

367   JNK inhibitor SP600125 or the DLK inhibitor, GNE-3511, blocked HSV reactivation
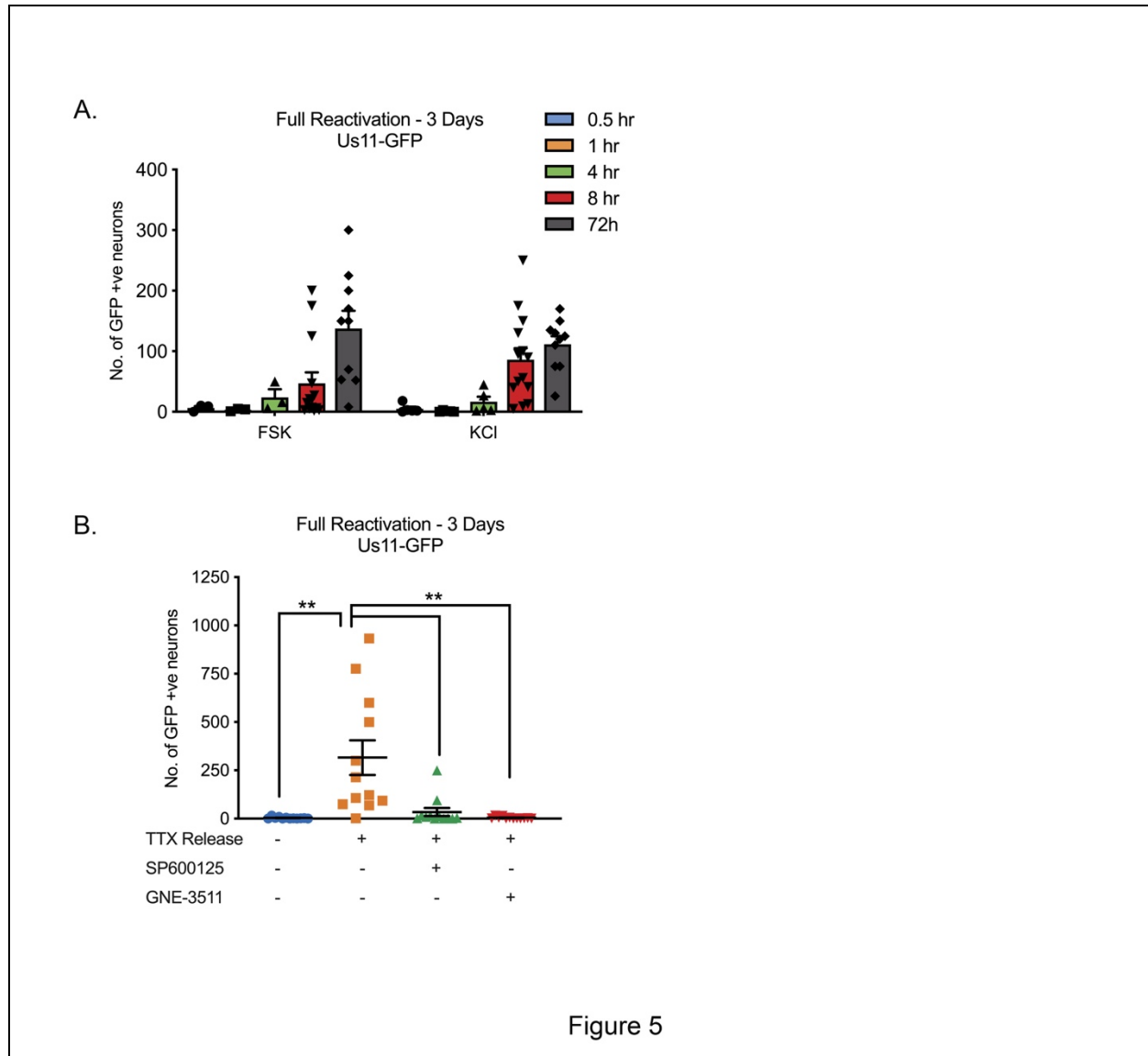
Figure 5

Figure 5. HSV Reactivation Triggered by Prolonged Neuronal Hyperexcitability is DLK/JNK Dependent. (A) Latently infected SCG cultures were treated with forskolin or KCl (55mM) for the indicated times followed by wash-out. Reactivation was quantified by number of Us11-GFP positive neurons at 3 days after the initial stimulus was added. (B) Latently infected neurons were placed in tetrodotoxin (TTX; 1μM) for 2 days and the TTX was then washed out. At the time of wash-out the JNK inhibitor SP600125 (20μM) or DLK inhibitor GNE-3511 (4μM) was added. Reactivation was quantified at 3-days post-wash-out. Individual experimental replicates are represented. Statistical comparisons were made using Welch's t-test.

368

369

370   following TTX-release. Therefore, directly inducing neuronal hyperexcitability triggers

371   HSV reactivation in a DLK/JNK-dependent manner.

372

373   <u>IL-1β Triggers HSV Reactivation in Mature Neurons in a DLK and HCN Channel</u>

374   <u>Dependent Manner</u>

375   Our data thus far point to a reactivation of HSV following increasing episodes of

376   neuronal hyperexcitability in a way that is requires activation of the JNK-cell stress

377   pathway. However, we wished to link this response to a physiological trigger that may

378   stimulate HSV reactivation *in vivo*. Increased HCN-channel activity has been associated

379   to inflammatory pain resulting from the activity of pyrogenic cytokines on neurons[64]. In

380   addition, IL-1β is known to act on certain neurons to induce neuronal excitation[39-41]. IL-

381   1β is released in the body during times of chronic, psychological stress. In addition, IL-

382   1β contributes to the fever response[31-34]. In sympathetic neurons, we found that

383   exposure of mature neurons to IL-1β induced an accumulation of the hyperexcitability-

384   associated histone post-translational modifications γH2AX and H3K9me3/S10p (Figure

385   6A-C). We did not observe the same changes for post-natal neurons. The reasons for

386   this maturation-dependent phenotype are unknown at this point but we hypothesize it

387   could be due to changes in the expression of cellular factors required to respond to IL-

388   1β. Therefore, these experiments were carried out on neurons that we more than 28

389   days old. The kinetics of induction of these histone modifications was different from

390   what we had previously observed for forskolin treatment, as both γH2AX and

391   H3K9me3/S10p steadily accumulated to 20h post-treatment. This likely reflects the

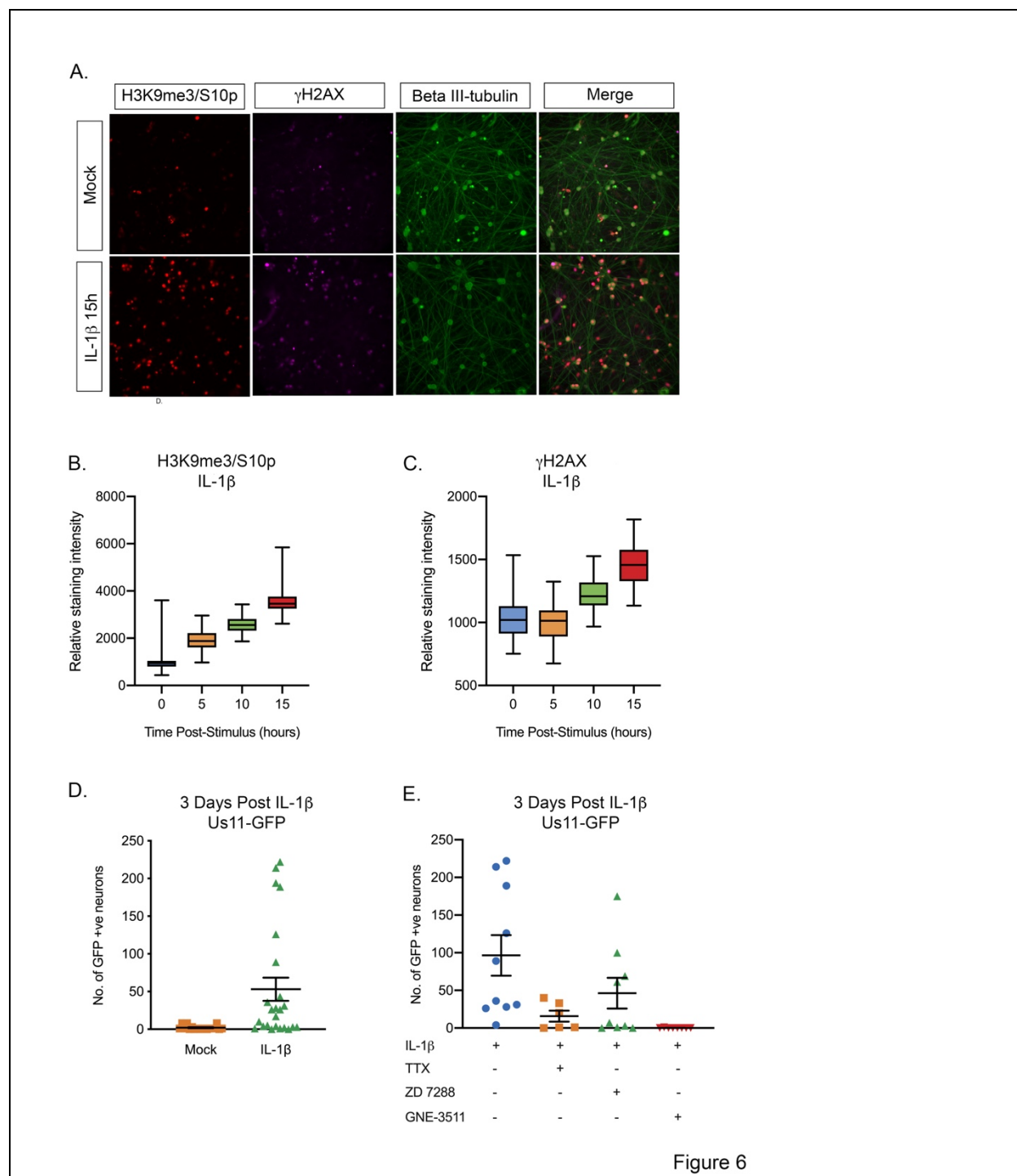392   activation of upstream signaling pathways in response to IL-1β prior to inducing

Figure 6

Figure 6. IL-1β-Induced HSV Reactivation is Linked to Heightened Neuronal Activity and DLK Activation. (A) Adult P28 SCG neurons were treated with IL-1β (30ng/mL) for 15 hrs and stained for H3K9me3/S10p, γH2AX and beta II-tubulin to mark neurons. (B-C) Quantification of the intensity of H3K9me3/S10p and γH2AX in neuronal nuclei following forskolin treatment from two independent experiments. (D). Addition of IL-1β to latently infected cultures of mature SCG neurons triggers HSV reactivation. (E). Quantification of IL-1β induced reactivation in the presence of the voltage gated sodium channel blocker TTX (1μM), the

HCN channel blocker ZD 7288 (10μM) and the DLK inhibitor GNE-3511 (4μM). In D and E individual experimental replicates are represented. Statistical comparisons were made using or two-tailed unpaired t-test (B, C) or Welch's t-test (D, E)

393

394   neuronal excitation as IL-1β increases the expression of voltage-gated sodium

395   channels[41]. Importantly, IL-1β was able to trigger HSV reactivation in mature neurons

396   (Figure 5D). Reactivation was reduced in the presence of the HCN-channel inhibitor ZD

397   7288 and the voltage-gated sodium channel inhibitor TTX (Figure 6F), indicating that IL-

398   1β triggered reactivation via increasing neuronal activity. Importantly, addition of the

399   DLK inhibitor GNE-3511 blocked reactivation in response to IL-1β (Figure 6F).

400   Therefore, IL-1β can induce HSV reactivation that is both dependent on neuronal

401   activity and induction of the JNK neuronal cell stress response.

402

403   Discussion

404   As herpesviruses hide in the form of a latent infections of specific cell types, they

405   sense changes to the infected cell that trigger the re-expression of viral lytic genes to

406   promote reactivation. HSV establishes latency in neurons and has previously been

407   found to sense changes in the neuronal stress signaling pathway to induce reactivation

408   from latency. As an excitable cell type, the function of neurons is to rapidly transmit

409   stimuli via the firing of action potentials, and under conditions of hyperexcitability,

410   neurons increase their propensity to fire repeated action potentials. Here we show that

411   this state of hyperexcitability induces HSV to undergo reactivation in a DLK/JNK

412   dependent manner, indicating that the virus responds to both activation of cell stress

413   signaling and prolonged hyperexcitability via a common pathway to result in

414   reactivation. This common pathway also permits viral lytic gene expression from

415   silenced promoters without the requirement of histone demethylase activity via a histone

416   phospho/methyl switch. Conditions that result in hyperexcitability include prolonged

417   periods of stress and inflammation, which are both linked to the release of IL-1β[31-34].

418   Consistent with this, here we show that IL-1β induces DNA damage, and histone H3

419   phosphorylation in sympathetic neurons, which are both markers of neuronal

420   excitability. Importantly, IL-1β triggered HSV reactivation that was dependent on

421   neuronal activity and activation of DLK. Therefore, this study identifies a physiological

422   stimulus that induces HSV reactivation via increasing neuronal excitability and places

423   DLK/JNK signaling and a histone phospho/methyl switch as central to HSV reactivation.

424

425   Neuronal hyperexcitability results in DNA damage followed by repair, which

426   together are thought to mediate the expression of cellular immediate early genes[29,30].

427   Here we show that forskolin treatment and IL-1β also induce DNA damage in

428   sympathetic neurons. Previously, HSV reactivation has been found to occur following

429   inhibition of DNA damage, inhibition of repair and exogenous DNA damage[12]. In the

430   context of repair inhibition or exogenous DNA damage, reactivation was dependent on

431   dephosphorylation of AKT by the PHLPP1 phosphatase and activation of JNK, and

432   therefore feeds into the same pathway as PI3K-inhibition. However, we did not observe

433   decreased AKT phosphorylation in response to forskolin treatment, indicating that the

434   mechanism of reactivation is distinct following physiological levels of DNA damage

435   resulting from neuronal hyperexcitability versus perturbation of the damage/repair

436   pathways.

437

438   Conditions that result in hyperexcitability include prolonged periods of stress and

439   inflammation, which are both linked to the release of IL-1β[31-34]. Consistent with these

440   findings, we show that IL-1β treatment induces two markers of neuronal excitability,

441   DNA damage and histone H3 phosphorylation, in primary sympathetic neurons. The IL-

442   1 family of cytokines act via the IL-1 receptor to activate downstream signaling

443   pathways [65]. IL-1β is released systemically during prolonged periods of psychological

444   stress and upon infection via activation of the inflammasome[31-34]. IL-1α, which also

445   signals via the IL-1R, is released locally as an alarmin. Interesting IL-1α and IL-1β are

446   found at high levels in keratinocytes and are released upon HSV-1 infection[42], where

447   they can mediate antiviral responses in underlying stromal fibroblasts and endothelial

448   cells. Antiviral responses mediated by IL-1 signaling have been found to involve NF-κB,

449   IRF3 and/or IRF1[43]. The downstream signaling elicited by IL-1 in neurons has not been

450   clearly defined and likely varies between different subtypes of neurons. NF-κB has been

451   reported to be absent in certain subtypes of neurons but constitutively active in

452   others[66,67], and a recent study suggests that NF-κB levels increase with neuronal

453   maturation[68], which may be why we only observed IL-1-mediated reactivation in mature

454   neurons. Additional studies have found a role for p38MAPK signaling and AKT/mTOR

455   signaling in neuronal IL-1-mediated responses[69,70]. A common feature of IL-1 signaling

456   in neurons is increased excitability, which has been associated with neurotransmitter

457   release, and mediates a variety of physiological responses including behavior

458   modulation and an intersection with the hosts' immune response[39-41]. IL-1 is also

459   associated with pathological conditions, including neurodegenerative disease such as

460   Alzheimer's disease[71]. There are multiple studies linking HSV-1 infection to the

461 progression of Alzheimer's[2]; therefore, the combination of both HSV infection and

462 increased IL-1 could have a feed forward effect on the progression of Alzheimer's

463 disease by promoting increased reactivation of HSV from latency.

464

465   Experiments using primary neuronal *in vitro* model systems and inducing

466 reactivation by PI3-kinase inhibition have shown that reactivation progresses over two

467 phases. Phase 1 involves the synchronous up-regulation of lytic gene expression that

468 occurrs independently of the viral transactivator VP16 and the activity of cellular histone

469 demethylases[15,18]. A population of neurons progress to full reactivation (Phase II), which

470 is dependent on both VP16 and HDM activity[15,18]. We previously found that lytic gene

471 expression in Phase I is DLK/JNK dependent and is corelated with a JNK-dependent

472 histone methyl/phospho switch on lytic gene promoters[15]. Here we demonstrate that a

473 Phase 1 wave of viral gene expression that is dependent on activation of JNK but not

474 histone demethylases also occurs in response to neuronal hyperexcitability. The co-

475 localization of viral genomes with H3K9me3/pS10 indicates that a histone

476 methyl/phospho switch also permits lytic gene expression to occur following forskolin

477 treatment in a manner that is independent of HDM activity. This indicates that

478 reactivation proceeds via a Phase 1-wave of gene expression in response to multiple

479 different stimuli. However we note that there may be differences in the mechanism and

480 kinetics of reactivation with different stimuli and/or strains of HSV-1 as reactivation

481 triggered by axotomy may bypass Phase I[19,20] and reactivation induced in vivo by heat

482 shock with a more pathogenic strain of HSV triggered more rapid reactivation [72]. It will

483 be especially interesting to determine in the future whether there are differences in the

484   progression to reactivation with different strains of HSV. Ultimately, these reactivation

485   kinetics may relate differences in the epigenetic structures of viral genomes that vary

486   based on virus strains or differential manipulation of host-cell signaling pathways.

487

488   The Wilcox lab demonstrated in 1992 that reactivation can be induced by

489   forskolin, and it has since been used as a trigger in multiple studies[25-28]. However, the

490   mechanism by which increasing levels of cAMP induces lytic gene expression was not

491   known. Here we link cAMP-induced reactivation to the excitation state of the neuron and

492   show that the initial induction of viral gene expression is dependent on DLK and JNK

493   activity but independent of CREB and PKA. The activity of PKA may be required for full

494   reactivation, which is also consistent with a role for PKA in overcoming repression of the

495   related Pseudorabies Virus during *de novo* axonal infection[73]. Our data also suggest

496   that CREB may be involved in the progression to full reactivation. However, the

497   mechanism of action of the inhibitor used here, 666-15, is not entirely clear. It has been

498   reported as preventing CREB-mediated gene expression, but may act to prevent

499   recruitment of histone acetyltransferases[74]. Therefore, inhibition of Phase II reactivation

500   by 666-15 would be consistent with more large-scale chromatin remodeling on the viral

501   genome at this stage. In addition, previous work has identified a role for inducible cAMP

502   early repressor (ICER) in HSV reactivation[26]. ICER is a repressor of gene expression

503   via heterodimerization with members of the CREB/ATF family of transcription factors.

504   CREB expression is also known to be down-regulated by loss of NGF-signaling[75].

505   Therefore, it is conceivable that inhibition, rather than activation, of CREB is important

506   for reactivation of HSV from latency.

507

508   Previously, we found that JNK activation by DLK is required for reactivation

509   following interruption of the NGF-signaling pathway. Here we find that forskolin and IL-

510   1β-mediated reactivation also required both DLK activity, further reinforcing the central

511   role of DLK and JNK in reactivation of HSV from latency. DLK is known as a master

512   regulator of neuronal response to stress stimuli and mediates whole cell death, axon

513   pruning, regeneration or generation depending on the nature of the stimuli. However, it

514   has not before been linked to neuronal hyperexcitability or the response to IL-1β

515   signaling. The known mechanisms of DLK activation include loss of AKT activation and

516   phosphorylation by PKA, neither of which could be linked to HSV reactivation mediated

517   by forskolin in this study. Following activation by DLK, one mechanism by which JNK is

518   thought to permit lytic gene expression is via recruitment to viral promoters and histone

519   phosphorylation. However, it is likely that there are additional, JNK-dependent effects

520   including activation of pioneer or transcription factors that also mediate viral gene

521   expression. Further insight into how HSV has hijacked this cellular pathway to induce

522   lytic gene expression may lead to novel therapeutics that prevent reactivation, in

523   addition to providing information on how viral gene expression initiates from promoters

524   assembled into heterochromatin.

525

526   <u>Acknowledgements</u>

529   (S.R.C. and J.B.S), NIH/NEI F30EY030397 (J.B.S), NIH/NIGMS T32GM008136 (S.D)

530   and T32GM007267 (J.B.S) and MRC (https://mrc.ukri.org) MC_UU_12014/5 (C.B).

531

532   **Materials and Methods**

533   **Reagents**

534   Compounds used in the study are as follows: Acycloguanosine, FUDR, Uridine,

535   SP600125, GNE-3511, GSK-J4, L-Glutamic Acid, and Ivabradine (Millipore Sigma);

536   Forskolin, LY 294002, 666-15, SQ 22536, KT 5720, Tetraethylammonium chloride,

537   Cesium chloride, OG-L002, S2101, Tetrotdotoxin, and ESI-09 (Tocris); 1,9-dideoxy

538   Forskolin, ZD 7288 and 8-bromo-cyclic AMP (Cayman Chemicals); Nerve Growth

539   Factor 2.5S (Alomone Labs); Primocin (Invivogen); Aphidicolin (AG Scientific); IL-1β

540   (Shenandoah Biotechnology); WAY-150138 was kindly provided by Pfizer, Dr. Jay

541   Brown and Dr. Dan Engel at the University of Virginia, and Dr. Lynn Enquist at

542   Princeton University. Compound information and concentrations used can be found

543   below in Table S1.

544

545   **Preparation of HSV-1 Virus Stocks**

546   HSV-1 stocks of eGFP-Us11 Patton were grown and titrated on Vero cells obtained

547   from the American Type Culture Collection (Manassas, VA). Cells were maintained in

548   Dulbecco's Modified Eagle's Medium (Gibco) supplemented with 10% FetalPlex

549   (Gemini Bio-Products) and 2 mM L-Glutamine. eGFP-Us11 Patton (HSV-1 Patton strain

550   with eGFP reporter protein fused to true late protein Us11[44]) was kindly provided by Dr.

551   Ian Mohr at New York University.

552

Primary Neuronal Cultures

Sympathetic neurons from the Superior Cervical Ganglia (SCG) of post-natal day 0-2

(P0-P2) or adult (P21-P24) CD1 Mice (Charles River Laboratories) were dissected as

previously described[15]. Rodent handling and husbandry were carried out under animal

protocols approved by the Animal Care and Use Committee of the University of Virginia

(UVA). Ganglia were briefly kept in Leibovitz's L-15 media with 2.05 mM L-Glutamine

before dissociation in Collagenase Type IV (1 mg/mL) followed by Trypsin (2.5 mg/mL)

for 20 minutes each at 37 ˚C. Dissociated ganglia were triturated, and approximately

10,000 neurons per well were plated onto rat tail collagen in a 24-well plate.

Sympathetic neurons were maintained in CM1 (Neurobasal® Medium supplemented

with PRIME-XV IS21 Neuronal Supplement (Irvine Scientific), 50 ng/mL Mouse NGF

2.5S, 2 mM L-Glutamine, and Primocin). Aphidicolin (3.3 µg/mL), Fluorodeoxyuridine

(20 µM) and Uridine (20 µM) were added to the CM1 for the first five days post-

dissection to select against proliferating cells.

Establishment and Reactivation of Latent HSV-1 Infection in Primary Neurons

Latent HSV-1 infection was established in P6-8 sympathetic neurons from SCGs.

Neurons were cultured for at least 24 hours without antimitotic agents prior to infection.

The cultures were infected with eGFP-Us11 (Patton recombinant strain of HSV-1

expressing an eGFP reporter fused to true late protein Us11). Neurons were infected at

a Multiplicity of Infection (MOI) of 7.5 PFU/cell (assuming 1.0×10^4 neurons/well/24-well

plate) in DPBS +$CaCl_2$ +$MgCl_2$ supplemented with 1% Fetal Bovine Serum, 4.5 g/L

575   glucose, and 10 µM Acyclovir (ACV) for three hours at 37 ˚C. Post-infection, inoculum

576   was replaced with CM1 containing 50 µM ACV for 5-6 days, followed by CM1 without

577   ACV. Reactivation was carried out in DMEM/F12 (Gibco) supplemented with 10% Fetal

578   Bovine Serum, Mouse NGF 2.5S (50 ng/mL) and Primocin. Inhibitors were added either

579   one hour prior to or concurrently with the reactivation stimulus. WAY-150138 (2-10

580   µg/mL) was added to reactivation cocktail to limit cell-to-cell spread. Reactivation was

581   quantified by counting number of GFP-positive neurons or performing Reverse

582   Transcription Quantitative PCR (RT-qPCR) of HSV-1 lytic mRNAs isolated from the

583   cells in culture.

584

585   **Analysis of mRNA expression by reverse-transcription quantitative PCR (RT-**

586   **qPCR)**

587   To assess relative expression of HSV-1 lytic mRNA, total RNA was extracted from

588   approximately $1.0x10^4$ neurons using the Quick-RNA™ Miniprep Kit (Zymo Research)

589   with an on-column DNase I digestion. mRNA was converted to cDNA using the

590   SuperScript IV First-Strand Synthesis system (Invitrogen) using equal amounts of RNA

591   (20-30 ng/reaction). To assess viral DNA load, total DNA was extracted from

592   approximately $1.0x10^4$ neurons using the Quick-DNA™ Miniprep Plus Kit (Zymo

593   Research). qPCR was carried out using *Power* SYBR™ Green PCR Master Mix

594   (Applied Biosystems). The relative mRNA or DNA copy number was determined using

595   the Comparative C_T ($\Delta\Delta C_T$) method normalized to mRNA or DNA levels in latently

596   infected samples. Viral RNAs were normalized to mouse reference gene GAPDH. All

597   samples were run in duplicate on an Applied Biosystems™ QuantStudio™ 6 Flex Real-

598   Time PCR System. Primers used are described in Table S2.

599

600   **Western Blot Analysis**

601   Neurons were lysed in RIPA Buffer with cOmplete, Mini, EDTA-Free Protease Inhibitor

602   Cocktail (Roche) and PhosSTOP Phosphatase Inhibitor Cocktail (Roche) on ice for one

603   hour with regular vortexing to aid lysis. Insoluble proteins were removed via

604   centrifugation, and lysate protein concentration was determined using the Pierce

605   Bicinchoninic Acid Protein Assay Kit (Invitrogen) using a standard curve created with

606   BSA standards of known concentration. Equal quantities of protein (generally 20-50 µg)

607   were resolved on 4-20% gradient SDS-Polyacrylamide gels (Bio-Rad) and then

608   transferred onto Polyvinylidene difluoride membranes (Millipore Sigma). Membranes

609   were blocked in PVDF Blocking Reagent for Can Get Signal (Toyobo) for one hour.

610   Primary antibodies were diluted in Can Get Signal Immunoreaction Enhancer Solution 1

611   (Toyobo) and membranes were incubated overnight at 4°C. Antibodies and

612   concentrations are described in Table S3 below. HRP-labeled secondary antibodies

613   were diluted in Can Get Signal Immunoreaction Enhancer Solution 2 (Toyobo) and

614   membranes were incubated for one hour at room temperature. Blots were developed

615   using Western Lightning Plus-ECL Enhanced Chemiluminescence Substrate

616   (PerkinElmer) and ProSignal ECL Blotting Film (Prometheus Protein Biology Products)

617   according to manufacturer's instructions. Blots were stripped for reblotting using

618   NewBlot PVDF Stripping Buffer (Licor).

619

Immunofluorescence

620

621 Neurons were fixed for 15 minutes in 4% Formaldehyde and blocked in 5% Bovine

622 Serum Albumin and 0.3% Triton X-100 and incubated overnight in primary antibody.

623 Antibodies and concentrations are described in Table S4 below. Following primary

624 antibody treatment, neurons were incubated for one hour in Alexa Fluor® 488-, 555-,

625 and 647-conjugated secondary antibodies for multi-color imaging (Invitrogen). Nuclei

626 were stained with Hoechst 33258 (Life Technologies). Images were acquired using an

627 sCMOS charge-coupled device camera (pco.edge) mounted on a Nikon Eclipse Ti

628 Inverted Epifluorescent microscope using NIS-Elements software (Nikon). Images were

629 analyzed and intensity quantified using ImageJ.

630

Click Chemistry

631

632 Click chemistry was carried out a described previously[53] with some modifications.

633 Neurons were washed with CSK buffer (10 mM HEPES, 100 mM NaCl, 300 mM

634 Sucrose, 3 mM $MgCl_2$, 5 mM EGTA) and simultaneously fixed and permeabilized for 10

635 minutes in 1.8% methonal-free formaldehyde (0.5% Triton X-100, 1%

636 phenylmethylsulfonyl fluoride (PMSF)) in CSK buffer, then washed twice with PBS

637 before continuing to the click chemistry reaction and immunostaining. Samples were

638 blocked with 3% BSA for 30 minutes, followed by click chemistry using EdC-labelled

639 HSV-1 DNA and the Click-iT EdU Alexa Flour 555 Imaging Kit (ThermoFisher Scientific,

640 C10638) according to the manufacturer's instructions. For immunostaining, samples

641 were incubated overnight with primary antibodies in 3% BSA. Following primary

642 antibody treatment, neurons were incubated for one hour in Alexa Fluor® 488-, 555-,

643   and 647-conjugated secondary antibodies for multi-color imaging (Invitrogen). Nuclei

644   were stained with Hoechst 33258 (Life Technologies). Images were acquired at 60x

645   using an sCMOS charge-coupled device camera (pco.edge) mounted on a Nikon

646   Eclipse Ti Inverted Epifluorescent microscope using NIS-Elements software (Nikon).

647   Images were analyzed and intensity quantified using ImageJ.

648

649   **Statistical Analysis**

650   Power analysis was used to determine the appropriate sample sizes for statistical

651   analysis. All statistical analysis was performed using Prism V8.4. Welch's t-test was

652   used for GFP fluorescence experiments and two-tailed unpaired t-test was used for RT-

653   qPCR and IF experiments; specific analyses are included in the figure legends. EdC

654   virus and H3K9me3S10/p co-localization was quantified using ImageJ after sample

655   blinding. Mean fluorescence intensity of γH2AX was quantified using ImageJ.

656

657

References

1   Arvin, A. *et al.* Human Herpesviruses: Biology, Therapy, and Immunoprophylaxis. (2007).

2   Itzhaki, R. F. Corroboration of a Major Role for Herpes Simplex Virus Type 1 in Alzheimer's Disease. *Front Aging Neurosci* **10**, 324, doi:10.3389/fnagi.2018.00324 (2018).

3   Suzich, J. B. & Cliffe, A. R. Strength in diversity: Understanding the pathways to herpes simplex virus reactivation. *Virology* **522**, 81-91, doi:10.1016/j.virol.2018.07.011 (2018).

4   Deshmane, S. L. & Fraser, N. W. During latency, herpes simplex virus type 1 DNA is associated with nucleosomes in a chromatin structure. *Journal of Virology* **63**, 943-947 (1989).

5   Wang, Q.-Y. *et al.* Herpesviral latency-associated transcript gene promotes assembly of heterochromatin on viral lytic-gene promoters in latent infection. *Proceedings of the National Academy of Sciences* **102**, 16055-16059 (2005).

6   Knipe, D. M. & Cliffe, A. Chromatin control of herpes simplex virus lytic and latent infection. *Nat Rev Microbiol* **6**, 211-221, doi:10.1038/nrmicro1794 (2008).

7   Cliffe, A. R., Garber, D. A. & Knipe, D. M. Transcription of the herpes simplex virus latency-associated transcript promotes the formation of facultative heterochromatin on lytic promoters. *J Virol* **83**, 8182-8190, doi:10.1128/JVI.00712-09 (2009).

8   Kwiatkowski, D. L., Thompson, H. W. & Bloom, D. C. The polycomb group protein Bmi1 binds to the herpes simplex virus 1 latent genome and maintains repressive histone marks during latency. *J Virol* **83**, 8173-8181, doi:10.1128/JVI.00686-09 (2009).

9   Wilcox, C. L. & Johnson, E. M. Characterization of nerve growth factor-dependent herpes simplex virus latency in neurons in vitro. *Journal of Virology* **62**, 393-399 (1988).

10   Wilcox, C. L., Smith, R. L., Freed, C. R. & Johnson, E. M. Nerve growth factor-dependence of herpes simplex virus latency in peripheral sympathetic and sensory neurons in vitro. *Journal of Neuroscience* **10**, 1268-1275 (1990).

11   Camarena, V. *et al.* Nature and duration of growth factor signaling through receptor tyrosine kinases regulates HSV-1 latency in neurons. *Cell Host Microbe* **8**, 320-330, doi:10.1016/j.chom.2010.09.007 (2010).

12   Hu, H.-L. *et al.* TOP2β-Dependent Nuclear DNA Damage Shapes Extracellular Growth Factor Responses via Dynamic AKT Phosphorylation to Control Virus Latency. *Molecular cell* **74**, 466-480.e464, doi:10.1016/j.molcel.2019.02.032 (2019).

13   Tedeschi, A. & Bradke, F. The DLK signalling pathway--a double-edged sword in neural development and regeneration. *EMBO reports* **14**, 605-614, doi:10.1038/embor.2013.64 (2013).

14   Geden, M. J. & Deshmukh, M. Axon degeneration: context defines distinct pathways. *Current opinion in neurobiology* **39**, 108-115, doi:10.1016/j.conb.2016.05.002 (2016).

15   Cliffe, A. R. *et al.* Neuronal Stress Pathway Mediating a Histone Methyl/Phospho Switch Is Required for Herpes Simplex Virus Reactivation. *Cell Host Microbe* **18**, 649-658, doi:10.1016/j.chom.2015.11.007 (2015).

16   Fischle, W. *et al.* Regulation of HP1–chromatin binding by histone H3 methylation and phosphorylation. *Nature* **438**, 1116-1122, doi:10.1038/nature04219 (2005).

17   Gehani, S. S. *et al.* Polycomb Group Protein Displacement and Gene Activation through MSK-Dependent H3K27me3S28 Phosphorylation. *Molecular Cell* **39**, 886-900, doi:10.1016/j.molcel.2010.08.020 (2010).

701   18   Kim, J. Y., Mandarino, A., Chao, M. V., Mohr, I. & Wilson, A. C. Transient reversal of
702   episome silencing precedes VP16-dependent transcription during reactivation of latent HSV-1 in
703   neurons. *PLoS Pathog* **8**, e1002540, doi:10.1371/journal.ppat.1002540 (2012).
704   19   Cliffe, A. R. & Wilson, A. C. Restarting Lytic Gene Transcription at the Onset of Herpes
705   Simplex Virus Reactivation. *J Virol* **91**, e01419-01416-01416, doi:10.1128/JVI.01419-16 (2017).
706   20   Liang, Y., Vogel, J. L., Narayanan, A., Peng, H. & Kristie, T. M. Inhibition of the histone
707   demethylase LSD1 blocks alpha-herpesvirus lytic replication and reactivation from latency. *Nat
708   Med* **15**, 1312-1317, doi:10.1038/nm.2051 (2009).
709   21   Liang, Y. *et al.* Targeting the JMJD2 histone demethylases to epigenetically control
710   herpesvirus infection and reactivation from latency. *Sci Transl Med* **5**, 167ra165,
711   doi:10.1126/scitranslmed.3005145 (2013).
712   22   Messer, H. G., Jacobs, D., Dhummakupt, A. & Bloom, D. C. Inhibition of H3K27me3-
713   specific histone demethylases JMJD3 and UTX blocks reactivation of herpes simplex virus 1 in
714   trigeminal ganglion neurons. *J Virol* **89**, 3417-3420, doi:10.1128/JVI.03052-14 (2015).
715   23   Hill, J. M. *et al.* Inhibition of LSD1 reduces herpesvirus infection, shedding, and
716   recurrence by promoting epigenetic suppression of viral genomes. *Sci Transl Med* **6**, 265ra169,
717   doi:10.1126/scitranslmed.3010643 (2014).
718   24   Noh, K.-M. *et al.* ATRX tolerates activity-dependent histone H3 methyl/phos switching to
719   maintain repetitive element silencing in neurons. *Proceedings of the National Academy of
720   Sciences* **112**, 201411258-201416827, doi:10.1073/pnas.1411258112 (2014).
721   25   Smith, R. L., Pizer, L. I., Johnson, E. M., Jr. & Wilcox, C. L. Activation of second-messenger
722   pathways reactivates latent herpes simplex virus in neuronal cultures. *Virology* **188**, 311-318,
723   doi:10.1016/0042-6822(92)90760-m (1992).
724   26   Colgin, M. A., Smith, R. L. & Wilcox, C. L. Inducible Cyclic AMP Early Repressor Produces
725   Reactivation of Latent Herpes Simplex Virus Type 1 in Neurons In Vitro. *Journal of Virology* **75**,
726   2912-2920, doi:10.1128/JVI.75.6.2912-2920.2001 (2001).
727   27   De Regge, N., Van Opdenbosch, N., Nauwynck, H. J., Efstathiou, S. & Favoreel, H. W.
728   Interferon Alpha Induces Establishment of Alphaherpesvirus Latency in Sensory Neurons In
729   Vitro. *PLoS ONE* **5**, e13076, doi:10.1371/journal.pone.0013076.t001 (2010).
730   28   Danaher, R. J., Jacob, R. J. & Miller, C. S. Herpesvirus quiescence in neuronal cells. V:
731   forskolin-responsiveness of the herpes simplex virus type 1 alpha0 promoter and contribution
732   of the putative cAMP response element. *J Neurovirol* **9**, 489-497,
733   doi:10.1080/13550280390218797 (2003).
734   29   Alt, F. W. & Schwer, B. DNA double-strand breaks as drivers of neural genomic change,
735   function, and disease. *DNA Repair (Amst)* **71**, 158-163, doi:10.1016/j.dnarep.2018.08.019
736   (2018).
737   30   Madabhushi, R. *et al.* Activity-Induced DNA Breaks Govern the Expression of Neuronal
738   Early-Response Genes. *Cell* **161**, 1592-1605, doi:10.1016/j.cell.2015.05.032 (2015).
739   31   Ericsson, A., Kovacs, K. J. & Sawchenko, P. E. A functional anatomical analysis of central
740   pathways subserving the effects of interleukin-1 on stress-related neuroendocrine neurons. *J
741   Neurosci* **14**, 897-913, doi:10.1523/jneurosci.14-02-00897.1994 (1994).
742   32   Goshen, I. & Yirmiya, R. Interleukin-1 (IL-1): a central regulator of stress responses. *Front
743   Neuroendocrinol* **30**, 30-45, doi:10.1016/j.yfrne.2008.10.001 (2009).

744   33   Koo, J. W. & Duman, R. S. Interleukin-1 receptor null mutant mice show decreased
745   anxiety-like behavior and enhanced fear memory. *Neurosci Lett* **456**, 39-43,
746   doi:10.1016/j.neulet.2009.03.068 (2009).
747   34   Saper, C. B. & Breder, C. D. The neurologic basis of fever. *N Engl J Med* **330**, 1880-1886,
748   doi:10.1056/NEJM199406303302609 (1994).
749   35   Glaser, R. & Kiecolt-Glaser, J. K. Chronic stress modulates the virus-specific immune
750   response to latent herpes simplex virus Type 1. *Annals of Behavioral Medicine* **19**, 78-82,
751   doi:10.1007/BF02883323 (1997).
752   36   Cohen, F. *et al.* Persistent stress as a predictor of genital herpes recurrence. *Archives of*
753   *internal medicine* **159**, 2430-2436 (1999).
754   37   Chida, Y. & Mao, X. Does psychosocial stress predict symptomatic herpes simplex virus
755   recurrence? A meta-analytic investigation on prospective studies. *Brain, behavior, and*
756   *immunity* **23**, 917-925, doi:10.1016/j.bbi.2009.04.009 (2009).
757   38   Roizman, B., Knipe, D. M. & Whitley, R.   (Lippincott Williams & Wilkins,
758   Philadelphia, 2013).
759   39   Vezzani, A. & Viviani, B. Neuromodulatory properties of inflammatory cytokines and
760   their impact on neuronal excitability. *Neuropharmacology* **96**, 70-82,
761   doi:10.1016/j.neuropharm.2014.10.027 (2015).
762   40   Schneider, H. *et al.* A neuromodulatory role of interleukin-1beta in the hippocampus.
763   *Proceedings of the National Academy of Sciences* **95**, 7778-7783 (1998).
764   41   Binshtok, A. M. *et al.* Nociceptors are interleukin-1beta sensors. *J Neurosci* **28**, 14062-
765   14073, doi:10.1523/JNEUROSCI.3795-08.2008 (2008).
766   42   Orzalli, M. H. *et al.* An Antiviral Branch of the IL-1 Signaling Pathway Restricts Immune-
767   Evasive Virus Replication. *Molecular Cell* **71**, 825-840.e826, doi:10.1016/j.molcel.2018.07.009
768   (2018).
769   43   Aarreberg, L. D. *et al.* Interleukin-1β Induces mtDNA Release to Activate Innate Immune
770   Signaling via cGAS-STING. *Molecular Cell*, doi:10.1016/j.molcel.2019.02.038 (2019).
771   44   Benboudjema, L., Mulvey, M., Gao, Y., Pimplikar, S. W. & Mohr, I. Association of the
772   Herpes Simplex Virus Type 1 Us11 Gene Product with the Cellular Kinesin Light-Chain-Related
773   Protein PAT1 Results in the Redistribution of Both Polypeptides. *Journal of Virology* **77**, 9192-
774   9203, doi:10.1128/jvi.77.17.9192-9203.2003 (2003).
775   45   Hoshi, T., Garber, S. S. & Aldrich, R. W. Effect of forskolin on voltage-gated K+ channels
776   is independent of adenylate cyclase activation. *Science* **240**, 1652-1655 (1988).
777   46   Kandel, E. R. The molecular biology of memory: cAMP, PKA, CRE, CREB-1, CREB-2, and
778   CPEB. *Mol Brain* **5**, 14, doi:10.1186/1756-6606-5-14 (2012).
779   47   de Rooij, J. *et al.* Mechanism of regulation of the Epac family of cAMP-dependent
780   RapGEFs. *J Biol Chem* **275**, 20829-20836, doi:10.1074/jbc.M001113200 (2000).
781   48   Gandia, L. *et al.* Differential effects of forskolin and 1,9-dideoxy-forskolin on nicotinic
782   receptor- and K+-induced responses in chromaffin cells. *Eur J Pharmacol* **329**, 189-199,
783   doi:https://doi.org/10.1016/S0014-2999(97)89180-7 (1997).
784   49   Haslam, R. J., Davidson, M. M. & Desjardins, J. V. Inhibition of adenylate cyclase by
785   adenosine analogues in preparations of broken and intact human platelets. Evidence for the
786   unidirectional control of platelet function by cyclic AMP. *Biochem J* **176**, 83-95,
787   doi:10.1042/bj1760083 (1978).

788   50   Patel, S. *et al.* Discovery of Dual Leucine Zipper Kinase (DLK, MAP3K12) Inhibitors with
789   Activity in Neurodegeneration Models. *Journal of Medicinal Chemistry* **58**, 141023155239000-
790   141023155239418, doi:10.1021/jm5013984 (2014).
791   51   van Zeijl, M. *et al.* Novel class of thiourea compounds that inhibit herpes simplex virus
792   type 1 DNA cleavage and encapsidation: resistance maps to the UL6 gene. *J Virol* **74**, 9054-9061,
793   doi:10.1128/jvi.74.19.9054-9061.2000 (2000).
794   52   Newcomb, W. W. & Brown, J. C. Inhibition of herpes simplex virus replication by WAY-
795   150138: assembly of capsids depleted of the portal and terminase proteins involved in DNA
796   encapsidation. *J Virol* **76**, 10084-10088, doi:10.1128/jvi.76.19.10084-10088.2002 (2002).
797   53   Alandijany, T. *et al.* Distinct temporal roles for the promyelocytic leukaemia (PML)
798   protein in the sequential regulation of intracellular host immunity to HSV-1 infection. *PLoS*
799   *Pathogens* **14**, e1006769-1006736, doi:10.1371/journal.ppat.1006769 (2018).
800   54   McFarlane, S. *et al.* The histone chaperone HIRA promotes the induction of host innate
801   immune defences in response to HSV-1 infection. *PLOS Pathogens* **15**, e1007667,
802   doi:10.1371/journal.ppat.1007667 (2019).
803   55   Kruidenier, L. *et al.* A selective jumonji H3K27 demethylase inhibitor modulates the
804   proinflammatory macrophage response. *Nature* **488**, 404-408, doi:10.1038/nature11262
805   (2012).
806   56   Sartiani, L., Mannaioni, G., Masi, A., Novella Romanelli, M. & Cerbai, E. The
807   Hyperpolarization-Activated Cyclic Nucleotide-Gated Channels: from Biophysics to
808   Pharmacology of a Unique Family of Ion Channels. *Pharmacol Rev* **69**, 354-395,
809   doi:10.1124/pr.117.014035 (2017).
810   57   Kullmann, P. H. *et al.* HCN hyperpolarization-activated cation channels strengthen
811   virtual nicotinic EPSPs and thereby elevate synaptic amplification in rat sympathetic neurons. *J*
812   *Neurophysiol* **116**, 438-447, doi:10.1152/jn.00223.2016 (2016).
813   58   DiFrancesco, D. & Tortora, P. Direct activation of cardiac pacemaker channels by
814   intracellular cyclic AMP. *Nature* **351**, 145-147, doi:10.1038/351145a0 (1991).
815   59   Kase, D. & Imoto, K. The Role of HCN Channels on Membrane Excitability in the Nervous
816   System. *J Signal Transduct* **2012**, 619747, doi:10.1155/2012/619747 (2012).
817   60   Ibata, K., Sun, Q. & Turrigiano, G. G. Rapid synaptic scaling induced by changes in
818   postsynaptic firing. *Neuron* **57**, 819-826, doi:10.1016/j.neuron.2008.02.031 (2008).
819   61   Turrigiano, G. G., Leslie, K. R., Desai, N. S., Rutherford, L. C. & Nelson, S. B. Activity-
820   dependent scaling of quantal amplitude in neocortical neurons. *Nature* **391**, 892-896,
821   doi:10.1038/36103 (1998).
822   62   Lee, H. K. & Kirkwood, A. Mechanisms of Homeostatic Synaptic Plasticity in vivo. *Front*
823   *Cell Neurosci* **13**, 520, doi:10.3389/fncel.2019.00520 (2019).
824   63   Sokolova, I. V. & Mody, I. Silencing-induced metaplasticity in hippocampal cultured
825   neurons. *J Neurophysiol* **100**, 690-697, doi:10.1152/jn.90378.2008 (2008).
826   64   Emery, E. C., Young, G. T., Berrocoso, E. M., Chen, L. & McNaughton, P. A. HCN2 ion
827   channels play a central role in inflammatory and neuropathic pain. *Science* **333**, 1462-1466,
828   doi:10.1126/science.1206243 (2011).
829   65   Weber, A., Wasiliew, P. & Kracht, M. Interleukin-1 (IL-1) pathway. *Sci Signal* **3**, cm1,
830   doi:10.1126/scisignal.3105cm1 (2010).

831 66   Listwak, S. J., Rathore, P. & Herkenham, M. Minimal NF-kappaB activity in neurons.
832 *Neuroscience* **250**, 282-299, doi:10.1016/j.neuroscience.2013.07.013 (2013).
833 67   Kaltschmidt, B. & Kaltschmidt, C. NF-kappaB in the nervous system. *Cold Spring Harb*
834 *Perspect Biol* **1**, a001271, doi:10.1101/cshperspect.a001271 (2009).
835 68   Yeh, J. X., Park, E., Schultz, K. L. W. & Griffin, D. E. NF-kappaB Activation Promotes
836 Alphavirus Replication in Mature Neurons. *J Virol* **93**, e01071-01019, doi:10.1128/JVI.01071-19
837 (2019).
838 69   Qian, J. *et al.* Interleukin-1R3 mediates interleukin-1-induced potassium current increase
839 through fast activation of Akt kinase. *Proc Natl Acad Sci U S A* **109**, 12189-12194,
840 doi:10.1073/pnas.1205207109 (2012).
841 70   Srinivasan, D., Yen, J. H., Joseph, D. J. & Friedman, W. Cell type-specific interleukin-1beta
842 signaling in the CNS. *J Neurosci* **24**, 6482-6488, doi:10.1523/JNEUROSCI.5712-03.2004 (2004).
843 71   Mrak, R. E. & Griffin, W. S. Interleukin-1, neuroinflammation, and Alzheimer's disease.
844 *Neurobiol Aging* **22**, 903-908, doi:10.1016/s0197-4580(01)00287-1 (2001).
845 72   Doll, J. R., Hoebe, K., Thompson, R. L. & Sawtell, N. M. Resolution of herpes simplex virus
846 reactivation in vivo results in neuronal destruction. *PLoS Pathog* **16**, e1008296,
847 doi:10.1371/journal.ppat.1008296 (2020).
848 73   Koyuncu, O. O., MacGibeny, M. A., Hogue, I. B. & Enquist, L. W. Compartmented
849 neuronal cultures reveal two distinct mechanisms for alpha herpesvirus escape from genome
850 silencing. *PLoS Pathogens* **13**, e1006608, doi:10.1371/journal.ppat.1006608 (2017).
851 74   Xie, F. *et al.* Identification of a Potent Inhibitor of CREB-Mediated Gene Transcription
852 with Efficacious in Vivo Anticancer Activity. *J Med Chem* **58**, 5075-5087,
853 doi:10.1021/acs.jmedchem.5b00468 (2015).
854 75   Riccio, A., Ahn, S., Davenport, C. M., Blendy, J. A. & Ginty, D. D. Mediation by a CREB
855 family transcription factor of NGF-dependent survival of sympathetic neurons. *Science* **286**,
856 2358-2361 (1999).

857

858

859

860

861

862

863

864

865

866

867   Supplemental Tables of Reagents

868   Table S1: Compounds Used and Concentrations

Compound	Supplier	Identifier	Concentration
Acycloguanosine	Millipore Sigma	A4669	10 µM, 50 µM
FUDR	Millipore Sigma	F-0503	20 µM
Uridine	Millipore Sigma	U-3003	20 µM
SP600125	Millipore Sigma	S5567	20 µM
GNE-3511	Millipore Sigma	533168	4 µM
GSK-J4	Millipore Sigma	SML0701	2 µM
L-Glutamic Acid	Millipore Sigma	G5638	3.7 µg/mL
Forskolin	Tocris	1099	60 µM
LY 294002	Tocris	1130	20 µM
666-15	Tocris	5661	2 µM
SQ 22,536	Tocris	1435	50 µM
KT 5720	Tocris	1288	3 µM
TEA	Tocris	3068	10 mM
CsCl	Tocris	4739	3 mM
OG-L002	Tocris	6244	15 µM, 30 µM
S2101	Tocris	5714	10 µM, 20 µM
Tetrodotoxin	Tocris	1069	1 µM
ESI-09	Tocris	4773	10 µM
ZD 7288	Cayman	15228	20 µM
8-bromo-cyclic AMP	Cayman	14431	125 µM

NGF 2.5S	Alomone Labs	N-100	50 ng/mL
Primocin	Invivogen	ant-pm-1	100 µg/mL
Aphidicolin	AG Scientific	A-1026	3.3 µg/mL
IL-1β	Shenandoah Bio.	100-167	30ng/mL
WAY-150138	Pfizer	NA	10 µg/mL

869

870

871 Table S2: Primers Used for RT-qPCR

872

Primer	Sequence 5' to 3'
mGAP 1SF	CAT GGC CTT CCG TGT GTT CCT A
mGAP 1SR	GCG GCA CGT CAG ATC CA
ICP27 F	GCA TCC TTC GTG TTT GTC ATT CTG
ICP27 R	GCA TCT TCT CTC CGA CCC CG
ICP8 1SF	GGA GGT GCA CCG CAT ACC
ICP8 1SR	GGC TAA AAT CCG GCA TGA AC
ICP4 F	TGC TGC TGC TGT CCA CGC
ICP4 R	CGG TGT TGA CCA CGA TGA GCC
UL30 F	CGC GCT TGG CGG GTA TTA ACA T
UL30 R	TGG GTG TCC GGC AGA ATA AAG C

UL48 F	TGC TCG CGA ATG TGG TTT AG
UL48 R	CTG TTC CAG CCC TTC ATG TT
gC #1 F	GAG TTT GTC TGG TTC GAG GAC
gC #1R	ACG GTA GAG ACT GTG GTG AA

873

874

875 Table S3: Antibodies Used for Western Blotting and Concentrations

876

Antibody	Supplier	Identifier	Concentration
Rb Phospho-Akt (S473)	CST	4060	1:500
Rb Akt (pan)	CST	C67E7	1:1000
Rb Phospho-c-Jun (S73)	CST	3270	1:500
Ms Monoclonal α-Tubulin	Millipore Sigma	T9026	1:2500
HRP Goat Anti-Rabbit IgG Antibody (Peroxidase)	Vector	PI-1000	1:10000
HRP Horse Anti-Mouse IgG Antibody (Peroxidase)	Vector	PI-2000	1:10000

877

878

879 Table S4: Antibodies Used for Immunofluorescence and Concentrations

880

Antibody	Supplier	Identifier	Concentration
Rb H3K9me3S10P	Abcam	ab5819	1:250
Ch Beta-III Tubulin	Millipore sigma	AB9354	1:1000
Ms γH2A.X	CST	80312S	1:100
Ms c-Fos	Novus	NB110-75039	1:125
F(ab')2 Goat anti Mouse IgG (H+L) Alexa Fluor® 647	Thermo Fisher	A21237	1:1000
F(ab') Goat anti Rabbit IgG (H+L) Alexa Fluor® 555	Thermo Fisher	A21425	1:1000
Goat anti Chicken IgY (H+L) Alexa Fluor® 647	abcam	ab150175	1:1000
Goat Anti-Chicken IgY H&L (Alexa Fluor® 488) preabsorbed	abcam	ab150173	1:1000
F(ab')2 Goat anti-Rabbit IgG (H+L) Alexa Fluor® 488)	Thermo Fisher	B40922	1:1000

881

882

883

884